Doctoral Dissertation

Functional Alteration of Family I.3 Lipase from *Pseudomonas* sp. MIS38 by "Lid Engineering"

(緑膿菌 MIS38 株由来ファミリーI.3 リパーゼのリッド エンジニアリングによる機能改変)

Maria Cheng

April 2014

International Program of Frontier Biotechnology
Division of Advanced Science and Biotechnology
Graduate School of Engineering
Osaka University

TABLE OF CONTENTS

CHAPTER 1

General introduction

1.1. Lipase

Lipase (EC 3.1.1.3) is defined as a carboxylesterase, which catalyses the hydrolysis (Fig. 1-1) and synthesis of long chain acylglycerols with triacylglycerol being the standard substrate (Jaeger & Eggert, 2002). This class of hydrolytic enzyme is widely produced by both eukaryotic and prokaryotic organisms, ranging from human, plant, animals, to microbes such as fungi, yeast and bacteria. Lipases play important physiological roles in digestion, processing and transport of lipids. Lipase-producing microbes usually secrete extracellular lipase to facilitate the absorption of lipid-containing nutrient. Pathogenic microbes secrete lipase as part of virulence factors responsible for infections (Stehr *et al*., 2003). Lipase genes are also found in virus, however, it has been suggested that these lipases play a nonenzymatic role, possibly in lipid binding only (Kamil *et al*., 2005).

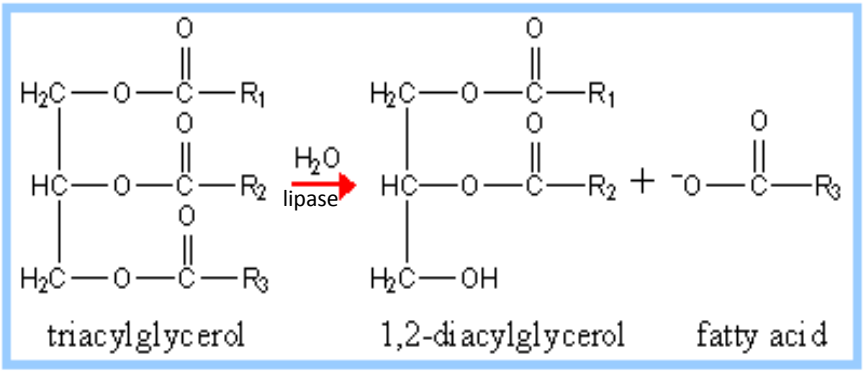

Fig. 1-1. Hydrolysis of triacylglycerol catalyzed by lipase, releasing diglyceride or monoglyceride and fatty acid. (http://www.rpi.edu/dept/bcbp/molbiochem/MBWeb/mb2/part1/lipoprot.htm).

True lipases undergo interfacial activation, in which the enzymatic activity significantly increases at saturated (micellar) substrate concentration. The presence of an amphiphilic lid, a surface loop covering the active site and controlling substrate access to active site is believed to be an important structural feature for interfacial activation (Cambillau *et al*., 1996), as shown in Figure 1-2. Upon contact with micellar substrates, this structure would move away, giving access to active site. Comparison of solved lipase crystal structures in the absence and presence of inhibitor/detergent revealed two forms of lipase: closed (lid covers the active site, inactive form)

and open (lid moves away from the active site, active form) conformations. It is in the open conformation that the enzyme is able to undergo interfacial activation (Brzozowski *et al*., 1991; Derewenda *et al*., 1992; van Tilbeurgh *et al.*, 1993; Angkawidjaja & Kanaya, 2006; Angkawidjaja *et al*., 2010). However, it is also worth stating that lipase which contains a lid structure but cannot undergo interfacial activation also presents (Verger, 1997), showing that exception to the generally accepted definition of true lipase also exists.

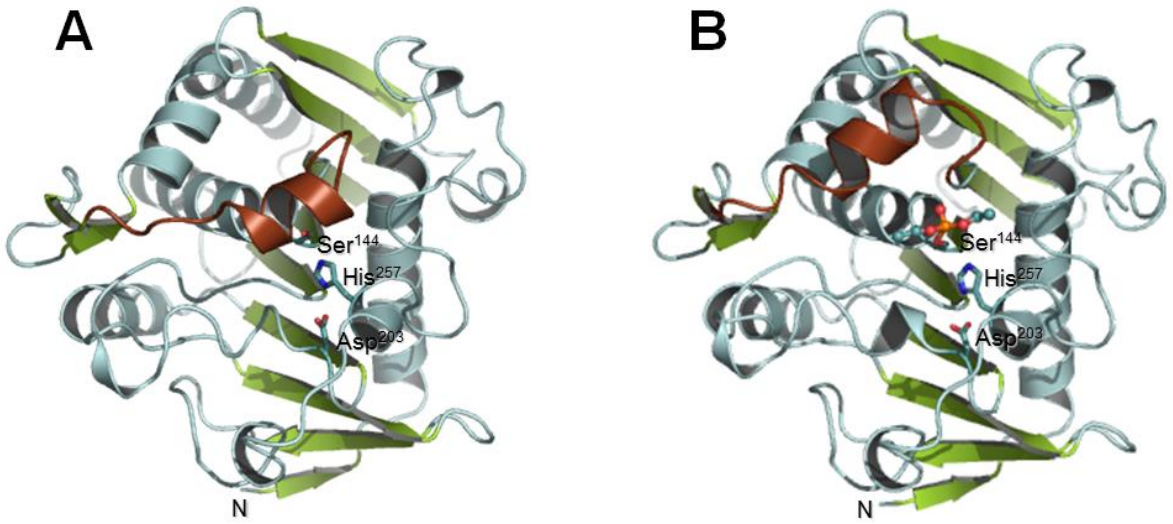

Fig. 1-2. Crystal structure of the closed (A) and open (B) conformations of a lipase from *Rhizomucor miehei*, a representative of the α/β hydrolase enzyme (PDB ID 3TGL and 4TGL, respectively). In the closed conformation (A), the 17-residue-long lid structure (shown in brown), which consists of amino acid residues 82–96, initially covers the active site that is composed of Ser144, Asp233 and His257 (shown in stick model). Upon binding of the inhibitor (shown in ball-and-stick model) to the active site, the lid is moved away from the active site, exposing the active site to the solvent (B) (Angkawidjaja & Kanaya, 2006).

Although it was nearly 100 years ago that microbiologist C. Eijkmann reported the ability of several bacteria in producing and secreting lipases, studies to develop lipases as ideal tools for organic chemist started when it was generally accepted that lipase is enzymatically active and stable in organic solvent (Jaeger & Eggert 2002; Arpigny & Jaeger, 1999). In micro-aqueous environments such as in organic solvent, instead of hydrolysis, lipase is capable to carry out various reactions, such as esterification, alcoholysis, aminolysis, and transesterification (Fig. 1-3). The high chemo-, regio-, and enantio-selectivities of lipase made it highly favorable for industrial applications, particularly in the production of enantiopure pharmaceuticals, agrochemicals, flavor compounds and other desired chiral compounds (Hasan *et al*., 2006).

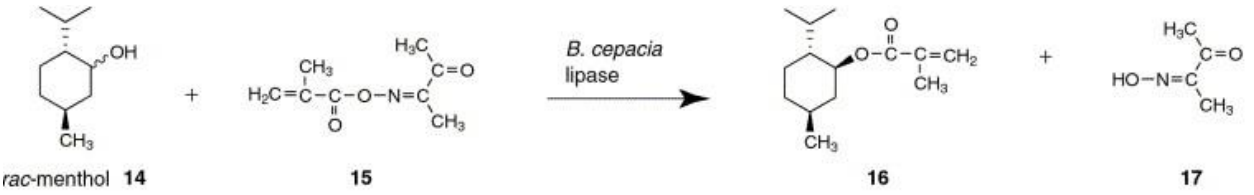

Fig. 1-3. Enantioselective synthesis of methyl methacrylate 16 (building block for polymerization for sustained released perfume) via transesterification by *Burkholderia cepacia* lipase (Jaeger & Eggert, 2002).

1.2. Active site and catalytic mechanism of lipase

Lipase is a member of the α/β hydrolase family, because all lipases share a common fold, termed α/β hydrolase fold (Angkawidjaja & Kanaya, 2006; Jaeger *et al*., 1999). Members of this large superfamily are structurally related but functionally diverged. The active site of the enzyme with an α/β hydrolase fold always contains a catalytic triad consisting of a nucleophilic residue, a catalytic acidic residue and a histidine residue. In lipases, the nucleophile is always Ser, whereas the catalytic acidic residue is Asp or Glu (Jaeger *et al*., 1999). Location of the nucleophilic serine residue is highly conserved, usually in a typical pentapeptide GxSxG motif. An example of the active site geometry with bound inhibitor is shown below (Fig. 1-4).

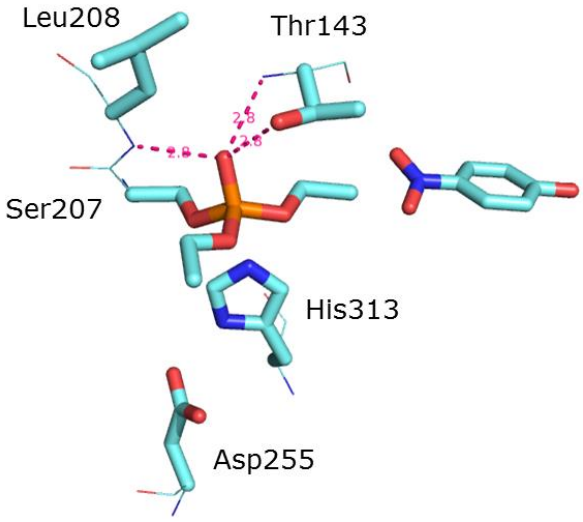

Fig. 1-4. Active site of *Pseudomonas* sp. MIS38 lipase with diethylphospho (DEP) group of inhibitor diethyl *p*-nitrophenyl phosphate (DENP) bound to the catalytic serine residue (Ser207) (PDB ID 3A70). Ser207, Asp255 and His313 form the catalytic triad, while Thr143 and Leu208 form the oxyanion hole. Broken red lines indicate the hydrogen bonds in the oxyanion hole, with their distances (Å) indicated. The side chain and main chain atoms are indicated by stick and line models, respectively. Oxygen, nitrogen and phosphorus atoms are colored red, dark blue and orange, respectively. A molecule of *p*-nitrophenol in the proximity of the active site is also shown.

Lipases have a Ser-His-Asp/Glu catalytic triad, which are similar to that observed in serine proteases. Therefore, the catalysis by lipases is thought to proceed in a similar manner as in serine proteases. The mechanism of substrate hydrolysis takes place in steps as described in Figure 1-5. Ser becomes nucleophilic because His draws a proton from the Ser hydroxyl group. This proton transfer can take place due to the presence of the catalytic acid (Asp/Glu) which precisely orients the imidazole ring of His and partly neutralizes the charge that develops on it (Jaeger *et al*., 1999).

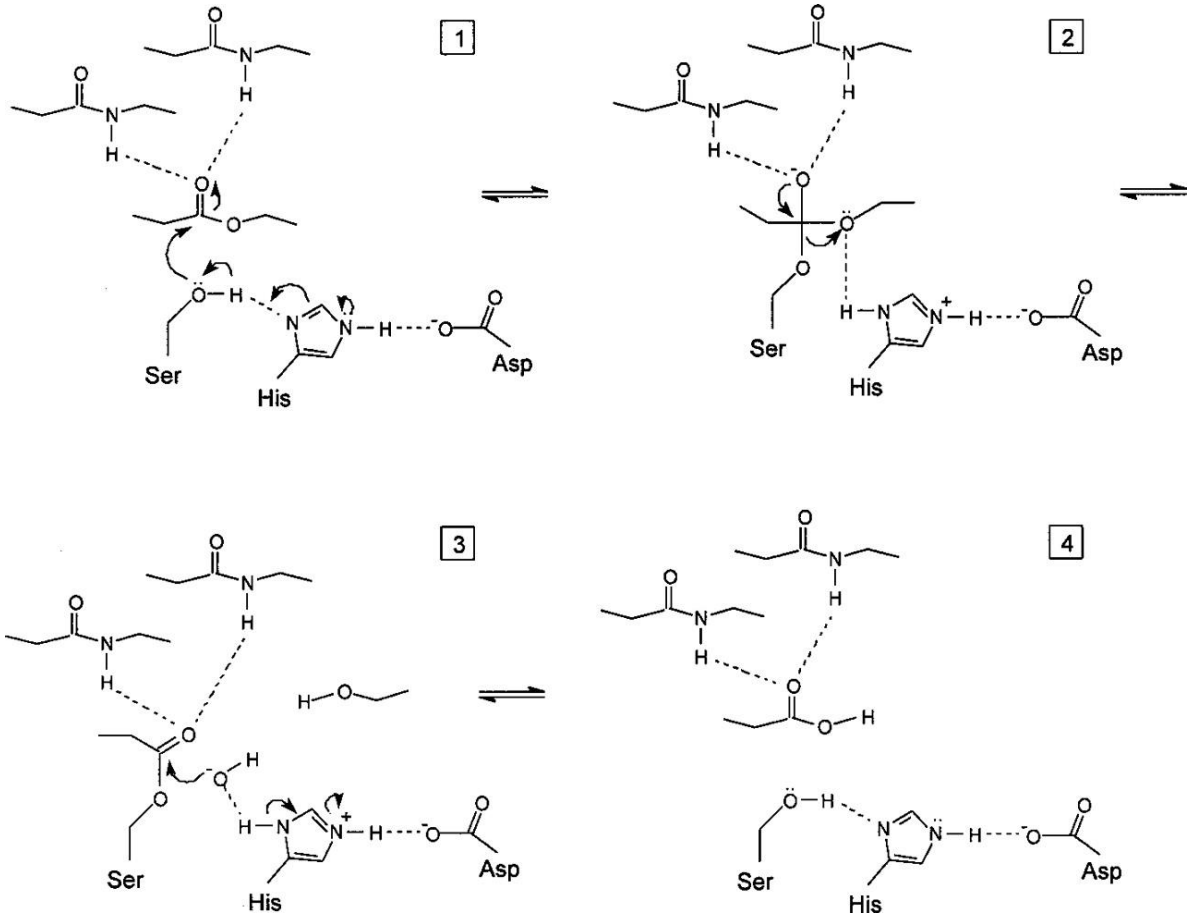

Fig. 1-5. Catalytic mechanism of lipases. (1) Binding of lipid, activation of nucleophilic Ser by neighboring His and nucleophilic attack of the substrate's carbonyl carbon atom by Ser O^-. (2) Transient tetrahedral intermediate, with O^-stabilized by interactions with two peptide NH groups. His donates a proton to the leaving alcohol component of the substrate. (3) The covalent intermediate ("acyl enzyme"), in which the acid component of the substrate is esterified to the enzyme's serine residue. The incoming water molecule is activated by neighboring His, and the resulting hydroxyl ion performs a nucleophilic attack on the carbonyl carbon atom of the covalent intermediate. (4) His donates a proton to the oxygen atom of the catalytic serine residue, the ester bond between Ser and acyl component is broken, and the acyl product is released (Jaeger *et al*., 1999).

Catalytic reaction takes place as the following. Carbonyl carbon of the lipid ester bond (in the substrate) is attacked by the nucleophilic oxygen atom of the catalytic serine residue, forming a transient tetrahedral intermediate. This intermediate is stabilized by hydrogen bonds between the oxyanion (negatively charged carbonyl oxygen atom) and at least two main-chain NH groups (the oxyanion hole). The proton in His is then donated to the ester oxygen of the susceptible bond to cleave it, resulting in the covalent intermediate of esterified Ser, with the alcohol component diffuses away. Next, His activates a water molecule by taking a proton from it, which allows the OH^- group to hydrolyze the covalent intermediate. Negatively charged tetrahedral intermediate is formed again, which is stabilized by interactions with the oxyanion hole. His then donates the proton to the oxygen atom of Ser, resulting in the release of acyl component.

1.3. Family I.3 lipase

Bacterial lipolytic enzymes are classified by Arpigny and Jaeger (1999) into eight families (families I-VIII), based on the amino acid sequences, biological properties, and available 3D structures. Among them, family I is the largest family which is further classified into seven subfamilies (I.1-I.7). Family I.1, I.2 and I.3 lipases are Gram-negative bacterial true lipases (Jaeger *et al*., 1999). Lipases from *Pseudomonas aeruginosa, P. fluorescens C9, P. fragi, Vibrio cholera* and *Acinetobacter calcoaceticus* are members of family I.1 lipase. Lipases from *P. luteola, Burkholderia cepacia, B. glumae* and *Chromobacterium viscosum* are members of family I.2 lipase. Family I.1 and I.2 lipases share similar structural features, secreted via type II secretion system (T2SS) and share relatively high amino acid sequence similarity (30-40%) (Arpigny & Jaeger, 1999). In contrast, family I.3 lipase is secreted via type I secretion system (T1SS), has higher molecular mass than family I.1 and I.2 lipases, and shows poor amino acid sequence similarities (<20%) to both family I.1 and I.2 lipases (Angkawidjaja & Kanaya, 2006; Arpigny & Jaeger, 1999). Molecular masses and optimum conditions for activities of representative members of family I.3 lipase are summarized in Table 1-1. Comparison of the amino acid sequences of representative members of family I.3 lipases (Fig. 1-6) shows that a typical pentapeptide GxSxG motif, and the active site residues are fully conserved.

Table 1-1. Members of family I.3 lipase with their properties (Angkawidjaja and Kanaya, 2006).

Producer strain	**GenBank accession no.**	**Molecular mass (kDa)**	**Optimum pH**	**Optimum temperature (°C)**	**Reference**
Pseudomonas sp. MIS38	AB025596	68	7.5	55	5
P. fluorescens B52 (LipB52)	AY623009	68	8.0	40	14
S. marcescens Sr41	D13253	65	8.0	45	15,16
S. marcescens SM6	U11258	65	NA	NA	17
P. fluorescens HU380	AB109033	64	8.5	45	18
P. fluorescens B52	M86350	50	NA	NA	19
Pseudomonas sp. KB700A	AB063391	50	8.0-8.5	35	20
P. fluorescens SIK W1	AF083061	50	8.5	45-55	21,22
P. fluorescens LS107d2	M74125	50	NA	NA	23

NA, not available

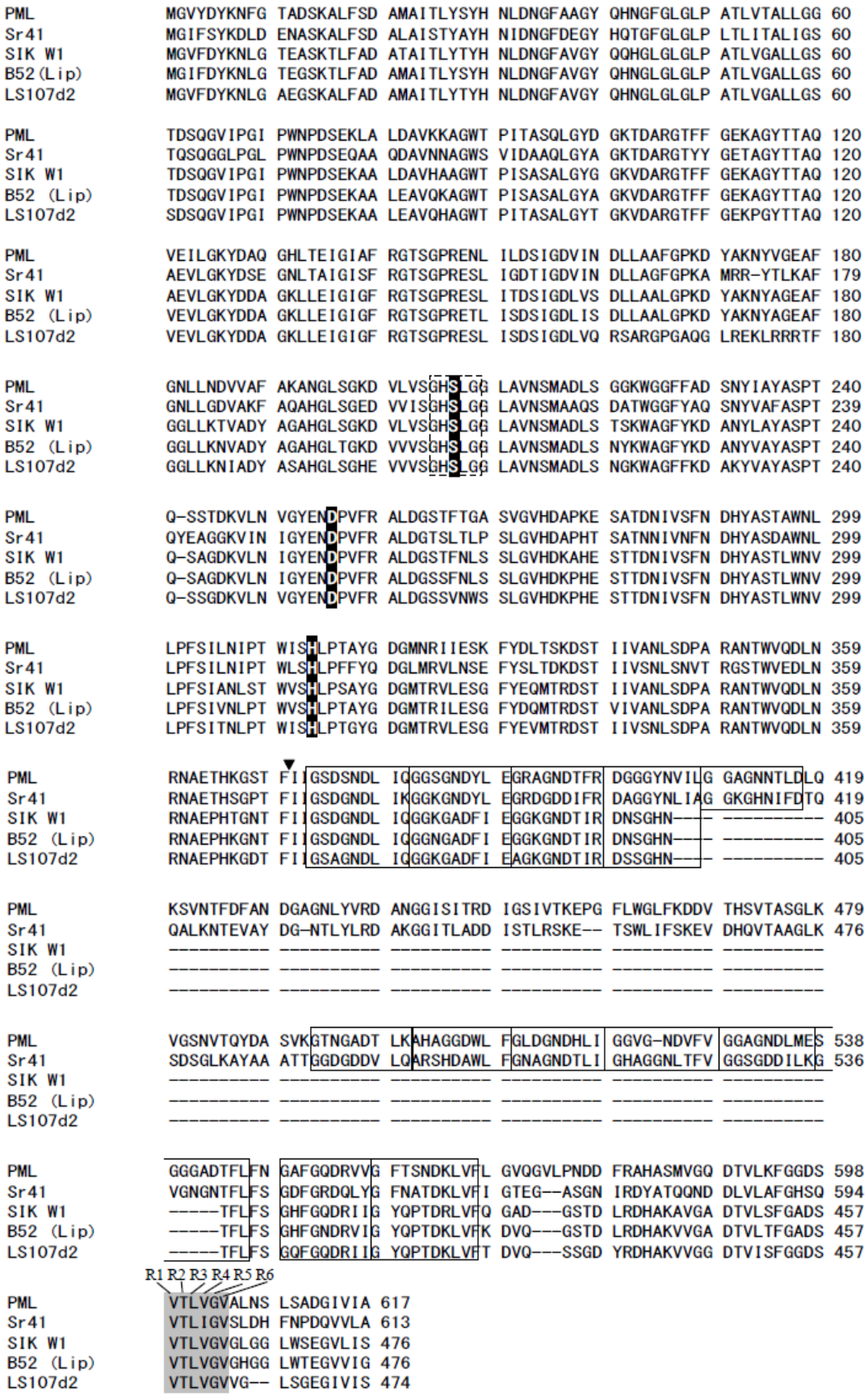
PML MGVYDYKNFG TADSKALFSD AMAITLYSYH NLDNGFAAGY QHNGFGLGLP ATLVTALLGG 60
Sr41 MGIFSYKDLD ENASKALFSD ALAISTYAYH NIDNGFDEGY HQTGFGLGLP LTLITALIGS 60
SIK W1 MGVFDYKNLG TEASKTLFAD ATAITLYTYH NLDNGFAVGY QQHGLGLGLP ATLVGALLGS 60
B52(Lip) MGIFDYKNLG TEGSKTLFAD AMAITLYSYH NLDNGFAVGY QHNGLGLGLP ATLVGALLGS 60
LS107d2 MGVFDYKNLG AEGSKALFAD AMAITLYTYH NLDNGFAVGY QHNGLGLGLP ATLVGALLGS 60
PML TDSQGVIPGI PWNPDSEKLA LDAVKKAGWT PITASQLGYD GKTDARGTFF GEKAGYTTAQ 120
Sr41 TQSQGGLPGL PWNPDSEQAA QDAVNNAGWS VIDAAQLGYA GKTDARGTYY GETAGYTTAQ 120
SIK W1 TDSQGVIPGI PWNPDSEKAA LDAVHAAGWT PISASALGYG GKVDARGTFF GEKAGYTTAQ 120
B52 (Lip) TDSQGVIPGI PWNPDSEKAA LEAVQKAGWT PISASALGYA GKVDARGTFF GEKAGYTTAQ 120
LS107d2 SDSQGVIPGI PWNPDSEKAA LEAVQHAGWT PITASALGYT GKVDARGTFF GEKPGYTTAQ 120
PML VEILGKYDAQ GHLTEIGIAF RGTSGPRENL ILDSIGDVIN DLLAAFGPKD YAKNYVGEAF 180
Sr41 AEVLGKYDSE GNLTAIGISF RGTSGPRESL IGDTIGDVIN DLLAGFGPKA MRR-YTLKAF 179
SIK W1 AEVLGKYDDA GKLLEIGIGF RGTSGPRESL ITDSIGDLVS DLLAALGPKD YAKNYAGEAF 180
B52 (Lip) VEVLGKYDDA GKLLEIGIGF RGTSGPRETL ISDSIGDLIS DLLAALGPKD YAKNYAGEAF 180
LS107d2 VEVLGKYDDA GKLLEIGIGF RGTSGPRESL ISDSIGDLVQ RSARGPGAQG LREKLRRRTF 180
PML GNLLNDVVAF AKANGLSGKD VLVSGHSLGG LAVNSMADLS GGKWGGFFAD SNYIAYASPT 240
Sr41 GNLLGDVAKF AQAHGLSGED VVISGHSLGG LAVNSMAAQS DATWGGFYAQ SNYVAFASPT 239
SIK W1 GGLLKTVADY AGAHGLSGKD VLVSGHSLGG LAVNSMADLS TSKWAGFYKD ANYLAYASPT 240
B52 (Lip) GGLLKNVADY AGAHGLTGKD VVVSGHSLGG LAVNSMADLS NYKWAGFYKD ANYVAYASPT 240
LS107d2 GGLLKNIADY ASAHGLSGHE VVVSGHSLGG LAVNSMADLS NGKWAGFFKD AKYVAYASPT 240
PML Q-SSTDKVLN VGYENDPVFR ALDGSTFTGA SVGVHDAPKE SATDNIVSFN DHYASTAWNL 299
Sr41 QYEAGGKVIN IGYENDPVFR ALDGTSLTLP SLGVHDAPHT SATNNIVNFN DHYASDAWNL 299
SIK W1 Q-SAGDKVLN IGYENDPVFR ALDGSTFNLS SLGVHDKAHE STTDNIVSFN DHYASTLWNV 299
B52 (Lip) Q-SAGDKVLN IGYENDPVFR ALDGSSFNLS SLGVHDKPHE STTDNIVSFN DHYASTLWNV 299
LS107d2 Q-SSGDKVLN VGYENDPVFR ALDGSSVNWS SLGVHDKPHE STTDNIVSFN DHYASTLWNV 299
PML LPFSILNIPT WISHLPTAYG DGMNRIIESK FYDLTSKDST IIVANLSDPA RANTWVQDLN 359
Sr41 LPFSILNIPT WLSHLPFFYQ DGLMRVLNSE FYSLTDKDST IIVSNLSNVT RGSTWVEDLN 359
SIK W1 LPFSIANLST WVSHLPSAYG DGMTRVLESG FYEQMTRDST IIVANLSDPA RANTWVQDLN 359
B52 (Lip) LPFSIVNLPT WVSHLPTAYG DGMTRILESG FYDQMTRDST VIVANLSDPA RANTWVQDLN 359
LS107d2 LPFSITNLPT WISHLPTGYG DGMTRVLESG FYEVMTRDST IIVSNLSDPA RANTWVQDLN 359
PML RNAETHKGST FIIGSDSNDL IQGGSGNDYL EGRAGNDTFR DGGGYNVILG GAGNNTLDLQ 419
Sr41 RNAETHSGPT FIIGSDGNDL IKGGKGNDYL EGRDGDDIFR DAGGYNLIAG GKGHNIFDTQ 419
SIK W1 RNAEPHTGNT FIIGSDGNDL IQGGKGADFI EGGKGNDTIR DNSGHN---- ---------- 405
B52 (Lip) RNAEPHKGNT FIIGSDGNDL IQGGNGADFI EGGKGNDTIR DNSGHN---- ---------- 405
LS107d2 RNAEPHKGDT FIIGSAGNDL IQGGKGADFI EAGKGNDTIR DSSGHN---- ---------- 405
PML KSVNTFDFAN DGAGNLYVRD ANGGISITRD IGSIVTKEPG FLWGLFKDDV THSVTASGLK 479
Sr41 QALKNTEVAY DG-NTLYLRD AKGGITLADD ISTLRSKE-- TSWLIFSKEV DHQVTAAGLK 476
SIK W1 ---------- ---------- ---------- ---------- ---------- ----------
B52 (Lip) ---------- ---------- ---------- ---------- ---------- ----------
LS107d2 ---------- ---------- ---------- ---------- ---------- ----------
PML VGSNVTQYDA SVKGTNGADT LKAHAGGDWL FGLDGNDHLI GGVG-NDVFV GGAGNDLMES 538
Sr41 SDSGLKAYAA ATTGGDGDDV LQARSHDAWL FGNAGNDTLI GHAGGNLTFV GGSGDDILKG 536
SIK W1 ---------- ---------- ---------- ---------- ---------- ----------
B52 (Lip) ---------- ---------- ---------- ---------- ---------- ----------
LS107d2 ---------- ---------- ---------- ---------- ---------- ----------
PML GGGADTFLFN GAFGQDRVVG FTSNDKLVFL GVQGVLPNDD FRAHASMVGQ DTVLKFGGDS 598
Sr41 VGNGNTFLFS GDFGRDQLYG FNATDKLVFI GTEG--ASGN IRDYATQQND DLVLAFGHSQ 594
SIK W1 -----TFLFS GHFGQDRIIG YQPTDRLVFQ GAD---GSTD LRDHAKAVGA DTVLSFGADS 457
B52 (Lip) -----TFLFS GHFGNDRVIG YQPTDKLVFK DVQ---GSTD LRDHAKVVGA DTVLTFGADS 457
LS107d2 -----TFLFS GQFGQDRIIG YQPTDKLVFT DVQ---SSGD YRDHAKVVGG DTVISFGGDS 457
R1 R2 R3 R4 R5 R6
PML VTLVGVALNS LSADGIVIA 617
Sr41 VTLIGVSLDH FNPDQVVLA 613
SIK W1 VTLVGVGLGG LWSEGVLIS 476
B52 (Lip) VTLVGVGHGG LWTEGVVIG 476
LS107d2 VTLVGVVG-- LSGEGIVIS 474

Fig. 1-6. Amino acid sequences of representative members of family I.3 lipase. The amino acid sequences of lipases from *Pseudomonas* sp. MIS38 (PML), *S. marcescens* Sr41 (Sr41), *P. fluorescens* SIK W1 (SIK W1), *P. fluorescens* B52 (B52 (lip)), and *P. fluorescens* LS107d2 (LS107d2) are aligned using the program CLUSTAL W (Thompson *et al*., 1994). The consensus GxSxG sequence, containing the active-site serine residue, is boxed by broken lines. The amino acid residues forming a catalytic triad, Ser, Asp, and His, are highlighted in black. The repetitive nine residue sequence motif, GGxGxDxux, is boxed by solid line. A putative C-terminal secretion signal (R1–R6) is shaded (Omori *et al*., 2001). The cleavage site with limited chymotryptic digestion (Amada *et al*., 2000) is shown by a solid arrowhead. Numbers represent the positions of the amino acid residues that start from the initiator methionine residue for each protein. The GenBank accession numbers for these sequences are listed in Table 1-1.

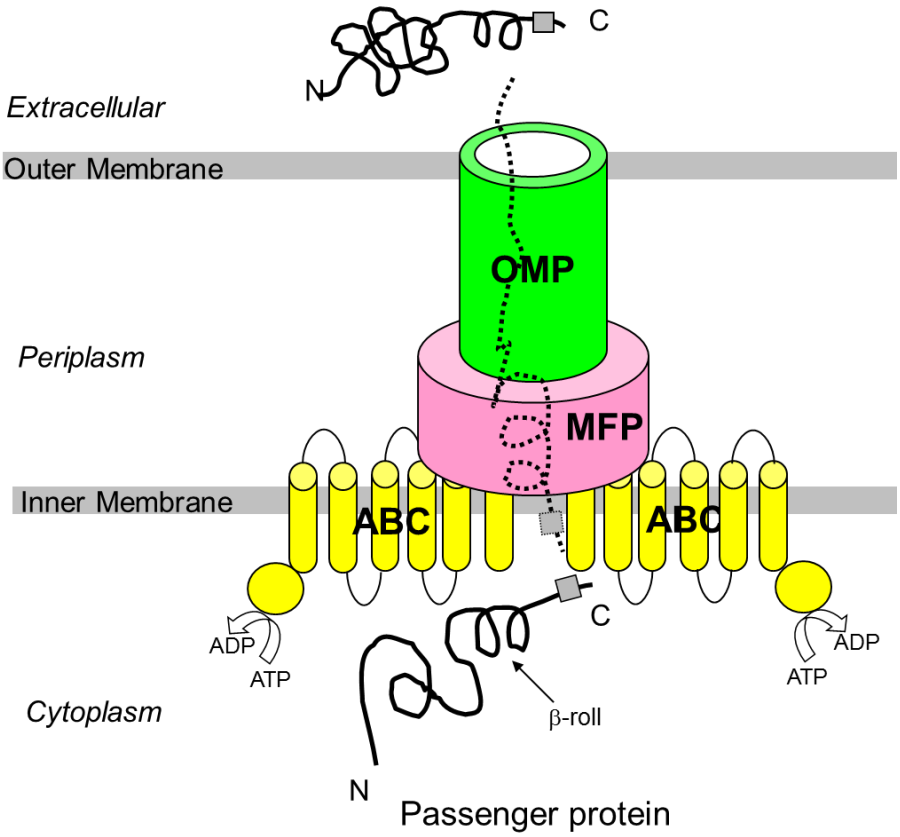

Fig. 1-7. A model of bacterial T1SS. ABC protein (white), membrane fusion protein (MFP; light gray), and outer membrane protein (OMP; dark gray) form a transporter complex protruding through the inner and outer membranes of Gram-negative bacteria. The secretion signal is shown by a gray box near the C-terminal end of the passenger protein. Protein secretion occurs in a single step, bypassing the periplasmic space directly to the extracellular medium (the direction of protein secretion is shown by a large shaded arrow). ATP hydrolysis by the ATPase domain of ABC protein provides energy for protein transport. The C-terminal secretion signal is recognized by the ABC protein, stimulating conformational change of the transporter complex and ATP hydrolysis, which leads to secretion of the passenger protein. A β-roll structure, formed by the repetitive sequences in the presence of calcium ions, is also shown (Angkawidjaja & Kanaya, 2006).

1.4. Type I secretion system (T1SS)

All of the members of family I.3 lipase are secreted out from the cell via T1SS. T1SS is a one-step secretion system in Gram-negative bacteria, used to transport the passenger protein from inside the cell directly to the environment. This transport system consists of three subunits, which are ATP-binding cassette (ABC) protein that binds ATP, membrane fusion protein (MFP) and outer membrane protein (OMP). These proteins form a channel that passes through the cell membrane, allowing the secretion of its passengers (Fig. 1-7). In Chapter 3, I used T1SS for lipase from *S. marcescens* SM8000 (Lip system), in which LipB is the ABC protein, LipC is MFP and LipD is OMP.

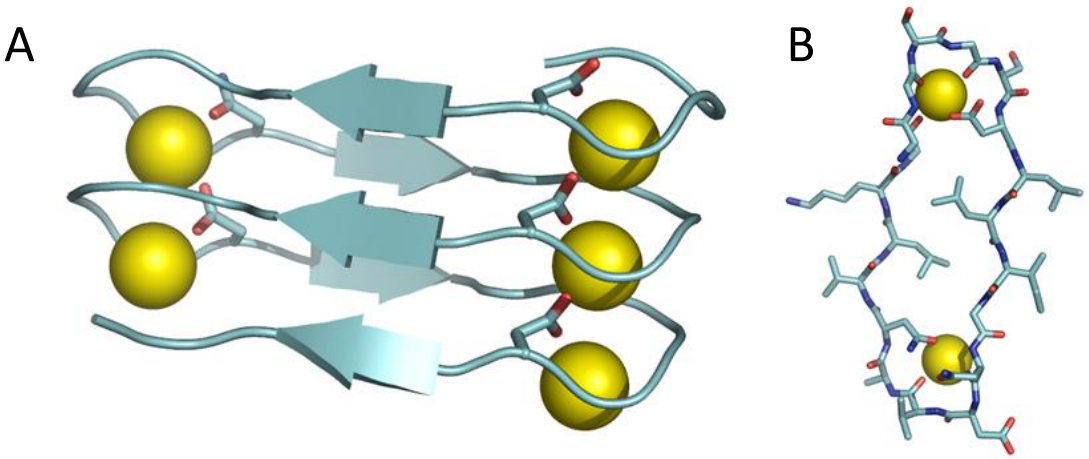

Fig. 1-8. (A) Side view of a β-roll structure. The β-roll structure formed by residues 333–379 of *P. aeruginosa* alkaline protease (PDBID 1AKL) is drawn by the program PYMOL. The β-strands and internally bound calcium ions are represented by arrows and yellow spheres, respectively. The side chains of the aspartate and asparagine residues, each of which provides two side-chain oxygen atom or one oxygen and one nitrogen atom for calcium binding, are shown in a stick model. (B) Top view of a β-roll structure. The first turn of the β-roll structure shown in *a* is shown in a stick model.

Passenger proteins of T1SS contain a C-terminal secretion signal with 50-60 residues, which remains intact after secretion (Angkawidjaja & Kanaya, 2006). On the upstream of this C-terminal secretion signal, a nine-residue sequence motif GGxGxDxux (x: any amino acid, u: hydrophobic amino acid) is repeated several times. This repetition is known as RTX (repeat in toxin) motif, glycine/aspartate-rich repeat region, or hemolysin-type calcium binding region. The RTX sequence is known for its role in calcium binding of some passenger proteins, and they form a β-roll motif (Fig. 1-8). The first six residues of this nine-residue motif forms a loop that

binds to calcium ion, while the last three residues forms a short β-strand (Fig. 1-8). The binding sites for calcium is provided by main chain carbonyl oxygen atoms of the glycine residues and the side chain oxygen atoms of the aspartate or asparagine residues (Fig. 1-8B).

1.5. *Pseudomonas* sp. MIS38 lipase (PML)

The nucleotide sequence of the *lip* gene encoding a lipase from *Pseudomonas* sp. MIS38 shows that PML is composed of 617 amino acid residues (Amada *et al*., 2000), with the molecular mass of 68 kDa. This nucleotide sequence is deposited in DDBJ with the accession number AB025596. The alignment of the amino acid sequences of family I.3 lipases (Fig. 1-6) shows that PML shares the amino acid sequence similarities of 95% to *P. fluorescens* HU380 lipase, 92% to *P. fluorescens* B52 (LipB52) lipase, 76% to *P. fluorescens* B52 lipase, 75% to *Pseudomonas* sp. KB700A lipase, 74% to *P. fluorescens* SIK W1 lipase, 72% to *P. fluorescens* LS107d2 lipase, and 61% to *S. marcescens* Sr41 and SM6 lipases (Angkawidjaja & Kanaya, 2006). Like any other passenger protein of T1SS, PML does not have any cysteine residue, indicating that PML, along with other members of family I.3 lipase, do not have a disulfide bond.

According to the limited proteolysis of PML (Amada *et al*., 2000) and the crystal structures in both closed (PDB ID 2Z8X) and open (PDB ID 2ZVD) conformations, PML consists of two domains. The N-domain (residues 1-372) contains the catalytic triad (Ser207, Asp255, His313) (Kwon *et al*., 2000), while the C-domain (residues 373-617) contains thirteen repeats of RTX motif and a secretion signal (Kuwahara *et al*., 2011). The C-domain is crucial not only for secretion but also for folding of the N-domain (Kwon *et al*., 2002; Angkawidjaja *et al*., 2005). According to the PML structure, thirteen RTX repeats form a β-roll sandwich structure, in which eight calcium ions bind. These calcium ions are required for folding of a β-roll sandwich motif (Amada *et al*., 2001; Angkawidjaja *et al*., 2006). Calcium-induced folding of RTX repeats may facilitate efficient secretion of PML by T1SS, as proposed for *Bordetella pertussis* adenylate cyclase (Chenal *et al*., 2009; Sotomayor *et al*., 2010). Structural and functional studies of PML have been done extensively, as described in more details in the following sections.

1.5.1. Crystal structures of PML

The first crystal structure of PML has been solved at 1.5Å resolution by the SIRAS method using a Pt-derivatized crystal of a cysteine mutant, in a closed conformation (PDB ID 2Z8X)

(Angkawidjaja *et al.*, 2007). The open conformation of PML has been solved at 2.1Å resolution by the molecular replacement method (Angkawidjaja *et al.*, 2010). This structure is similar to that of lipase from *S. marcescens* SM6 (SML) in the open conformation (Meier *et al.*, 2007). The first methionine residue is not be observed in both closed and open conformations of PML (Angkawidjaja *et al.*, 2007: Angkawidjaja *et al.*, 2010). Both structures show that the C-domain of PML has 13 repeats of RTX that form a β-roll sandwich, where eight calcium ions bind (Fig. 1-9).

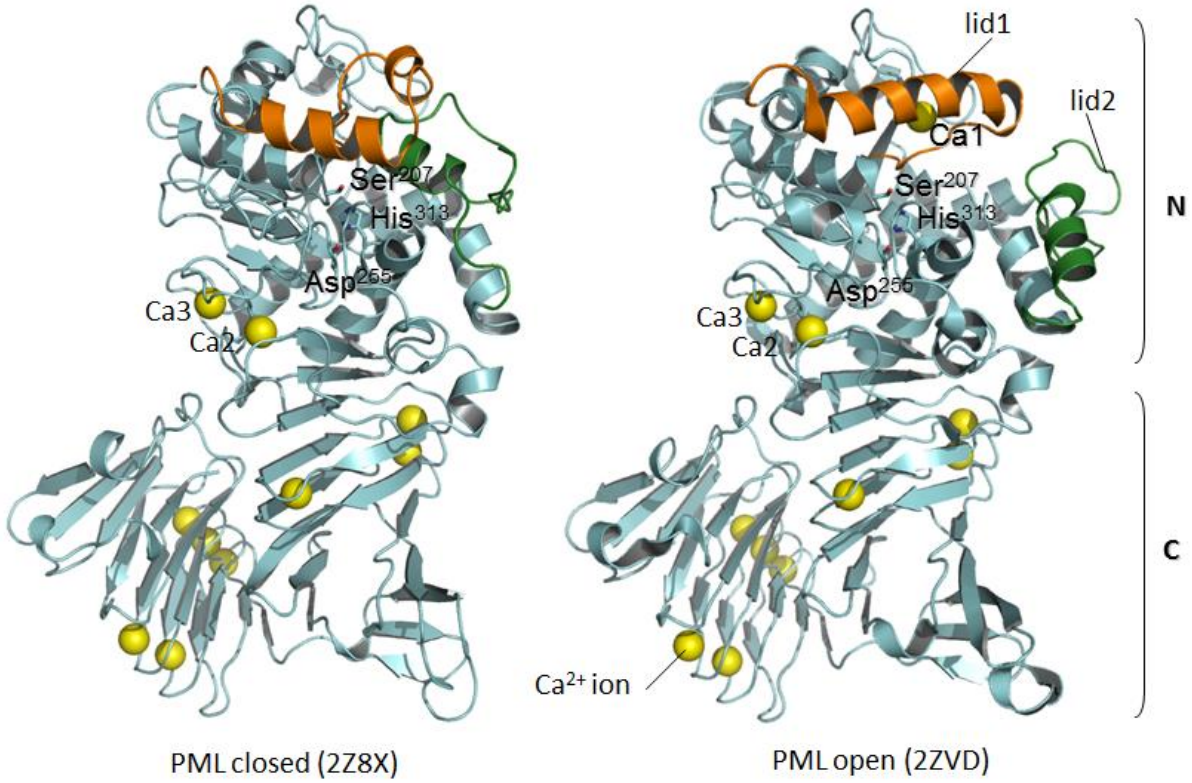

Fig. 1-9. Crystal structures of PML in closed (left panel) and open (right panel) conformations. N and C represent the N- and C- domains of PML. Calcium ions are shown in yellow spheres. Ca1, Ca2 and Ca3 at the N-domain are indicated. Lid1 and lid2 are colored orange and green, respectively. The active site residues (Ser207, Asp255, His313) are indicated by stick models.

Comparison between the closed and open conformations of PML shows that PML has two lid structures (Fig. 1-9). By analyzing the root mean square deviation (rmsd) value of each residue in the closed and open conformations, three regions were found to have significant differences (Fig.1-10B) (9). Two of them are lid1 (residues 146-167) and lid2 (residues 46-74), and the third region is identified as a flexible loop (residues 457-465).

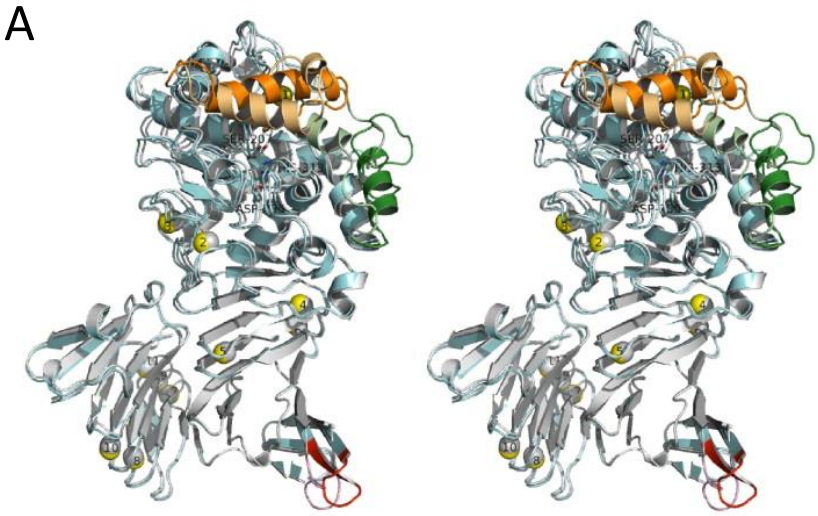

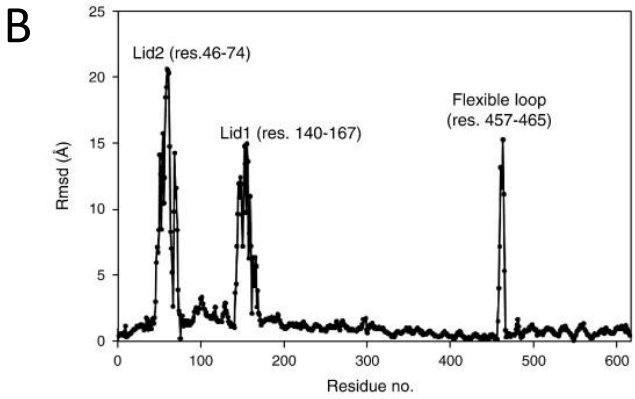
Lid2 (res.46-74)
Lid1 (res. 140-167)
Flexible loop
(res. 457-465)
Rmsd (Å)
Residue no.

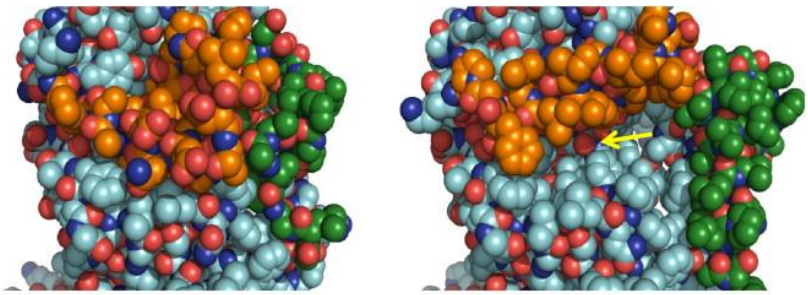
PML^Ca (closed)
PML^CaT (open)

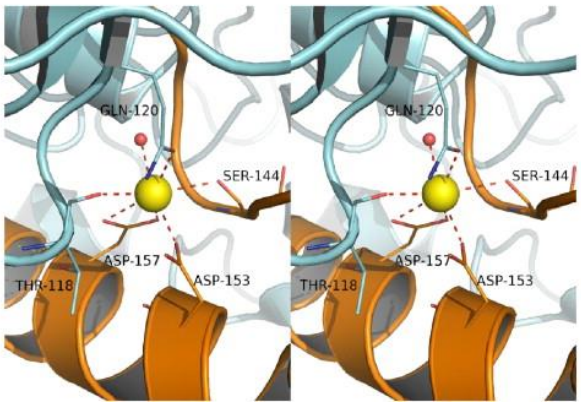
GLN-120
SER-144
ASP-157
ASP-153
THR-118

Fig. 1-10. (A) A stereo view of the superimposed structures of PML in the closed and open conformations. For the open conformation, the backbone is colored cyan, lid1 is colored orange, lid2 is colored green and a flexible loop is colored red. Eleven calcium ions are shown as yellow spheres, with their numbers indicated. Three active site residues (Ser207, Asp255 and His313) are indicated by stick models, in which the oxygen atoms are colored red and the nitrogen atoms are colored blue. The closed conformation, including 10 calcium ions, is colored gray, except that lid1 is colored light orange and lid2 is colored light green. (B) The C^{α} rmsd value of each residue between PML in the open conformation and PML in the closed conformation. Regions with significant displacements are indicated. (C) Space-filling models of PML in the closed and open conformations. The regions around the active sites of PML in the closed conformation and PML in the open conformation are shown. The reactive O^{γ} atom of Ser207 is indicated by a yellow arrow. Lid1 is colored orange, lid2 is colored green and other regions are colored cyan. The oxygen atoms are shown in red and the nitrogen atoms are shown in blue. (D) A stereo view of the Ca1 site of PML in the open conformation. The calcium ions are shown as a yellow sphere and the water molecule is shown as red sphere. The amino acid residues that are coordinated with the calcium ions are indicated by stick models in which the oxygen atoms are colored red and the nitrogen atoms are colored blue. Lid1 is colored orange and other regions are colored cyan.

Lid1 and lid2 assume amphiphilic helical structures. These lids have both hydrophilic and hydrophobic residues. One side of these lids contains the hydrophilic residues with several acidic residues, which are buried in the open conformation and exposed to the solvent in the closed conformation. The other side of these lids contains the hydrophobic residues which are solvent-exposed, interacting with the hydrophobic substrate in the open conformation, and buried inside the protein in the closed conformation. Since the crystal structure of PML in the open conformation is obtained in the presence of calcium ions and 0.02% Triton X-100 (Angkawidjaja *et al*., 2010), which mimics the condition in which the enzyme exhibits activity in the presence of substrate, it is obvious that lid displacements from closed-to-open occur, to facilitate binding to the hydrophobic substrate, by exposing the once buried hydrophobic residues to the solvent.

The third region with significant difference between the closed and open conformations is a flexible loop located at the C-domain of PML (Fig. 1-10A and B). Crystals of PML in an open conformation consist of two molecules per asymmetric unit. One molecule is intact and the flexible loop is visible, whereas the other molecule is not intact and the loop is disordered (Angkawidjaja *et al*., 2010). Therefore, the high flexibility of this loop may be caused by molecular packing in crystals.

Another difference between the closed and open conformations of PML is the Ca1 site. This site only exists in the open conformation (Fig. 1-9). Ca1 is hexacoordinated with the side chains of Asp157 (bidentate), Asp153 and Gln120 (monodentate), and main chain oxygen atoms

of Thr 118 and Ser 144 (Fig. 1-10D). A water molecule is also present, coordinating with Ca1. The Ca1 site is buried under lid1 with a long helical structure in the open conformation. In the closed conformation, this long helix does not exist, but is sharply bent to form a helix-turn-helix structure. The structure of lid1 is changed from a helix-turn-helix structure to a long helical structure when Ca1 binds to the protein (Fig. 1-9). It has been proposed that Ca1 acts as a "hook" to stabilize the open conformation of PML, since two negatively charged aspartate residues (Asp153 and Asp157) are located close to each other due to coordination with Ca1 (Fig. 1-10D). In the absence of calcium ions, these two aspartate residues may not be able to come close to each other due to negative charge repulsion.

The active site of PML is exposed to the solvent only when PML assumes an open conformation (Fig. 1-10C). The accessible surface areas (ASA) of the Oγ atom of Ser207 in the closed and open conformations are calculated to be 0.3 and 6.6Å, respectively (Angkawidjaja *et al*., 2010). In lipases, lid acts as a gate that allows the access of the substrate to the active site. Therefore, the displacement of lid1 and lid2 in PML is necessary to allow the access of the susbtrate to the active site and thereby to make the conformation of the active site active, where the catalytic reaction occurs.

1.5.2. Interfacial activation mechanism of PML

A combination of X-ray crystallography and molecular dynamics (MD) simulation has been used to investigate the interfacial activation mechanism of PML. Availability of the PML crystal structures in the closed, open and inhibitor-bound forms makes it possible to make a thorough structural analysis to explain how PML undergoes interfacial activation. MD simulation with PML in the open conformation without micelles (open-to-closed) shows that lid2 closes first, while lid1 maintains its open conformation (Angkawidjaja *et al*., 2010). Furthermore, MD simulation with PML in the closed conformation (closed-to-open) in the presence of micelles (in the absence of calcium) shows that lid1 opens, while lid2 remains closed. Taken together, these results suggest that upon interfacial activation, lid1 opens first upon binding of Ca1 that functions as a hook for stabilization of the fully open conformation of lid1, and lid2 opens subsequently (Angkawidjaja *et al*., 2010).

1.5.3. Role of calcium-binding sites in N-terminal domain of PML

The N-terminal domain of PML contains three calcium-binding sites. They are the Ca1, Ca2 and Ca3 sites (Fig. 1-9). The roles of these sites have been analyzed by constructing the single mutant proteins at the Ca1 (D157A-PML), Ca2 (D275A-PML) and Ca3 (D337A-PML) sites.

As mentioned earlier, the Ca1 site is formed when PML assumes an open conformation, in which lid1 is anchored by the calcium ion. Asp157 moves leftward by approximately 15Å to coordinate with this calcium ion. The mutation of Asp157 to Ala obviously removes the Ca1 site, since Asp 157 has a bidentate coordination with Ca1. D157A-PML does not exhibit lipase activity in the absence of calcium ions, but exhibits weak esterase activity (0.7% of that of PML, but higher than that of the active site mutant which is <0.06%) (Kuwahara *et al*, 2008), suggesting that Ca1 is necessary for lipase activity. Micellar substrate of lipase may be able to bind to the active site only when lid1 is fully open and is anchored by Ca1. However, the Ca1 site is not necessary for esterase activity, since the presence of substrate and nonionic detergent (e.g. Triton X-100) may allow dissociation of lid1 and lid2 from the active site (Kuwahara *et al.*, 2008). The dissociation constant of Ca1 has been determined to be 0.13 mM (Amada *et al*., 2001)

Ca2 is heptacoordinated by the side chains of Asp275, Asn284 (bidentate), Glu253, Asn284 (monodentate), main chain oxygen atom of Asp283, and two water molecules. Therefore, it is most likely that by mutating Asp275 to Ala (D275A-PML), the Ca2 site is lost. D175A-PML is less stable than PML by approximately 5^0C, and it exhibits weak lipase and esterase activities (Kuwahara *et al.*, 2008). Since all of the amino acid residues which coordinate with Ca2 are located in a large loop that also contains one of the active site residue, Asp255, it has been proposed that the Ca2 site is probably required to make the conformation of the active site fully active and stable (Kuwahara *et al.*, 2008). It has also been proposed that Ca2 is required to assist chaperone-like function of the β-roll motif, because Ca2 stabilizes β8-strand, which is located at the end of a long parallel β-sheet extended from one site of the first β-roll motif in the C-domain (Kuwahara *et al.*, 2008).

Ca3 is heptacoordinated by the side chain of Asp337 (bidentate), Asp283 (monodentate), main chain oxygen atoms of Lys278 and Ala 281, and two water molecules (Fig. 1-11A). These amino acid residues are not fully conserved in family I.3 lipases (Fig. 1-6), and the Ca3 site is not observed in the structure of SML (Meier *et al.*, 2007). According to the crystal structure of D337A-PML (Fig. 1-11B), the Ca3 site is not present in this protein. This protein is as active as PML, but is less stable than PML by approximately 5^0C, indicating that Ca3 contributes to the stabilization of PML.

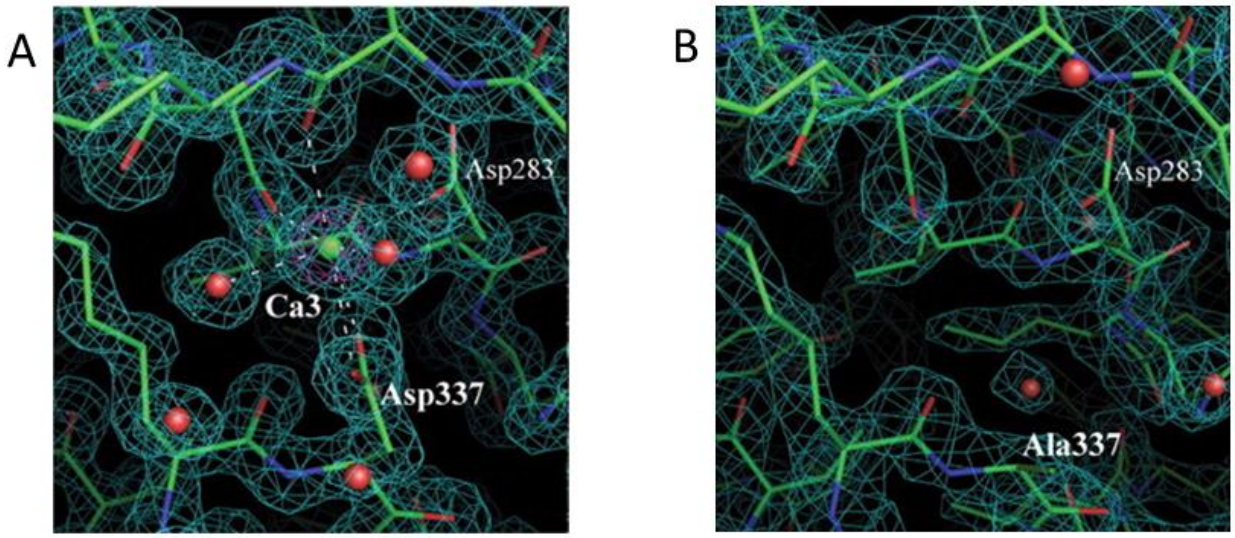

Fig. 1-11. (A) Electron density around the Ca3 site of PML. The 2Fo-Fc maps contoured at the 2.0σ and 8.0σ levels are shown in cyan and magenta, respectively. The coordinate bonds for Ca3 are represented by broken lines. (B) Electron density around residue 337 of D337A-PML (PDB ID 2ZJ6). The 2Fo-Fc map contoured at the 2.0σ level is shown. The calcium ion and water molecules are shown as green sphere, and red spheres, respectively. Protein backbone, oxygen and nitrogen atoms are colored green, red and blue, respectively (Kuwahara *et al.*, 2008).

1.5.4. The importance of RTX

The C-domain of PML contains 13 repeats of RTX motif and a secretion signal (Kuwahara *et al.*, 2011). These repetitive RTX motifs are folded into a β-roll sandwich structure upon binding of calcium ions (Amada *et al.*, 2001) (Fig. 1-9). The number of these repetitive RTX motifs can be reduced to six without significantly affecting the activity, stability, and secretion level of PML (Kwon *et al.*, 2002) (Fig. 1-12). Further reduction of this number greatly reduces the stability and secretion level, and thus abolishes the enzymatic activity of PML (Kwon *et al.*,

2002) (Fig. 1-12).The secretion level greatly decreases when the stability (resistance to chymotryptic digestion) greatly decreases, suggesting that the repetitive RTX motifs are necessary to make the protein stable inside the cell, prior to secretion via T1SS. Other members of family I.3 lipase such as lipases from *P. fluorescens* SIK W1, *P. fluorescens* LS107d2, and *P. fluorescens* KB700A have only five repeats of RTX motif (Fig. 1-6), suggesting that five repeats are enough to promote the folding of family I.3 lipase into an active and stable conformation (Angkawidjaja & Kanaya, 2006).

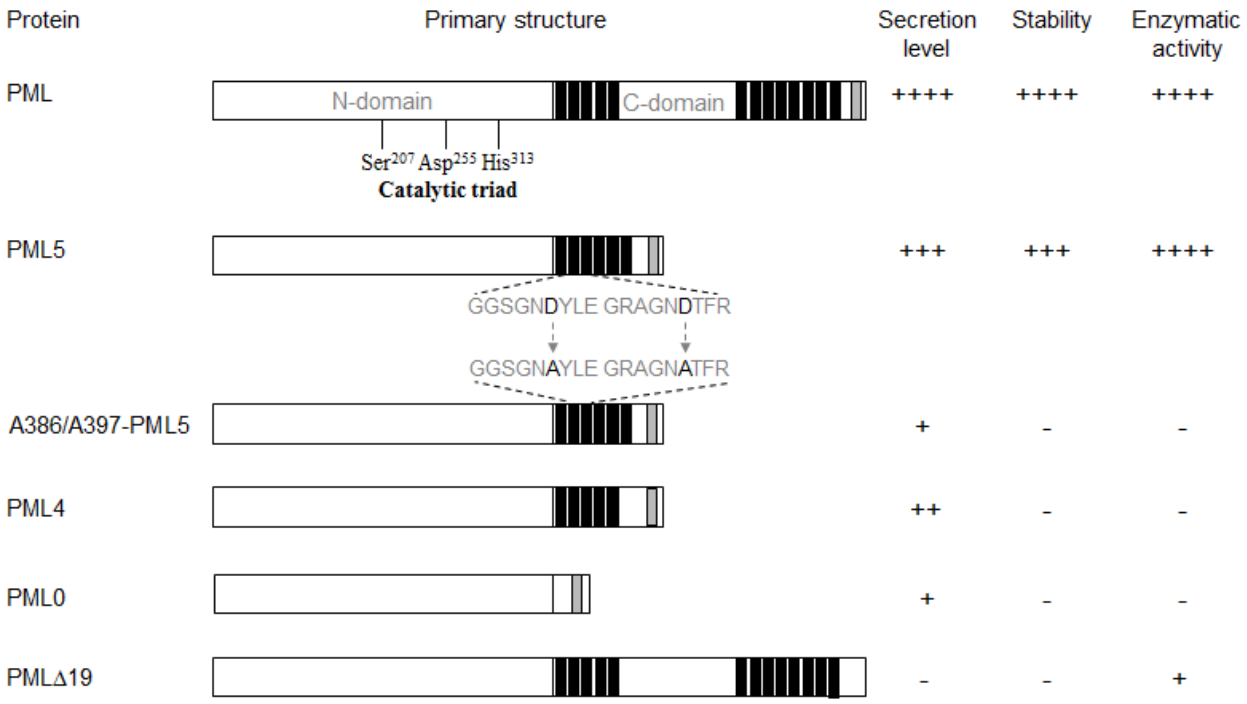

Fig. 1-12. Comparison of the secretion level, stability, and activity of *Pseudomonas* sp. MIS38 lipase (PML) and its variants (Amada *et al.*, 2001). The amino acid sequences of these proteins are schematically shown. In these sequences, the repetitive RTX motifs and the putative six-residue secretion signal are represented by solid and shaded boxes, respectively. The secretion level, stability (resistance to chymotryptic digestion), and enzymatic activity of each protein relative to those of PML are shown by ++++, +++, ++, +, and –, in which ++++ and – represent 'very high' and 'very low', respectively. Secretion of these proteins was examined using *E. coli* DH5 cells carrying the Lip system. Stability and activity of these proteins were examined using the refolded protein, which was overproduced in the *E. coli* cells in inclusion bodies, solubilized in the presence of urea, refolded, and purified. 'Enzymatic activity' represents the specific activity, which is defined as the enzymatic activity per milligram of protein. The specific activity of the refolded protein of PML was nearly identical to that of the secreted protein (Angkawidjaja & Kanaya, 2006).

The RTX motif has to be functional to carry out its structural role. Mutations of the aspartate residues within this motif to Ala seriously decrease the enzymatic activity and stability

of PML (Angkawidjaja *et al*., 2005; Angkawidjaja & Kanaya, 2006). The aspartate residues in the repeats are known to coordinate with the calcium ion, which assists correct folding of the repetitive RTX motifs to β-roll structure (Angkawidjaja *et al*., 2005). The reduced secretion efficiency of A386/A397-PML5 compared to PML5 suggests that less protein being secreted out due to less protein available for secretion (Fig. 1-12). A386/A397-PML5 is much less stable and susceptible to proteolytic degradation than PML, probably because a β-roll structure is not formed, or only partially formed.

As a member of family I.3 lipase, PML contains a C-terminal secretion signal within the C-terminal 19 residues. Truncation of these residues (PMLΔ19) results in a mutant protein lacking the ability to be secreted via T1SS, with increased susceptibility to chymotryptic digestion (Fig. 1-12) (Kwon *et al*., 2002). As a result, the enzymatic activity is also greatly decreased. Therefore, the C-terminal 19 residues are important not only for secretion of PML, but also to make the structure of PML stable and functional.

1.5.5. Role of the C-terminal secretion signal

A five-residue sequence motif, VTLVG (residues 15-19 from the last), and an extreme C-terminal motif, DGIVIA (residues 1-6 from the last), are located with the C-terminal 19 residues of PML (Fig. 1-13). These motifs are relatively well conserved in the passenger proteins of T1SS. 2A-PML, a mutant in which two of the five-residue sequence motif are changed to Ala (Fig. 1-13), shows significantly lower secretion level compared to that of PML (Kuwahara *et al*., 2011). On the other hand, the secretion level of 3A-PML, in which three of the extreme C-terminal motif are changed to Ala (Fig. 1-13), is comparable to that of PML. These results suggest that the five-residue sequence motif, instead of the extreme C-terminal motif, is important for secretion of PML.

Comparison of the thermal stability of these mutants and the PML derivatives without the C-terminal five (PMLΔ5) and ten (PMLΔ10) residues with that of PML shows that 3A-PML, PMLΔ5 and PMLΔ10 are less stable than PML by 2.1, 7.6 and 7.6^{0}C, respectively (Kuwahara *et al*., 2011). These results indicate that the extreme C-terminal region contributes to the

stabilization of PML. The enzymatic activity of PML is not seriously affected by these mutations and truncations (Kuwahara *et al*., 2011).

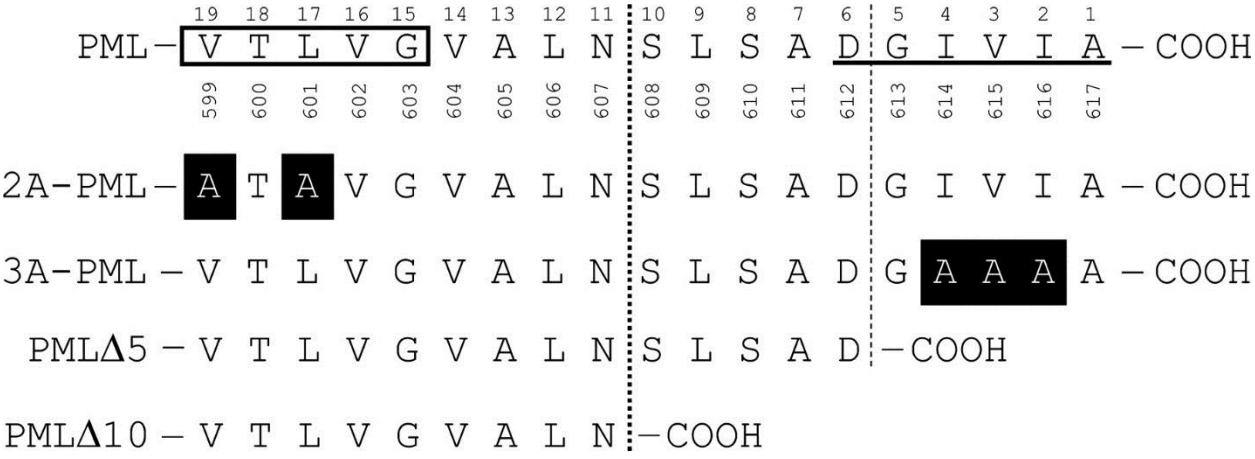

Fig. 1-13. The amino acid sequences of the C-terminal regions of PML and its mutant proteins. Numbers below and above the sequence of PML represent the positions of the amino acid residues starting from the N- and C-termini of PML, respectively. The mutated residues are denoted with white letters and black background. A five-residue sequence motif is boxed and an extreme C-terminal motif is underlined for the PML sequence.

1.6. Lid engineering in lipase

Protein engineering is a useful and indispensable tool in improving the activity, selectivity and also stability of target lipase, as well as altering its properties in tailoring a lipase with specific characteristic for specific purposes. Development of the method to alter the enzymatic properties of lipase is crucial because a condition, in which lipase is used for industrial purposes, is often quite different from its natural one. Therefore, optimization of the lipase function is necessary not only to increase the lipase activity, but also to broaden the range of lipase application.

One of the most widely used approach in engineering lipase is lid engineering, by which a lid structure of target lipase is changed by the mutation and/or deletion. Abundant amount of researches on lipases from various sources have shown that lid interacts with the substrate and controls the access of the substrate to the active site, and therefore contributes to substrate selectivity and specificity of lipase. Therefore, enzymatic properties of lipase can be easily altered by mutating the lid region of lipase, changing its amino acid sequence, swapping lid, or deleting part/all of the lid structure, as shown by previous studies using lipases from human

(Jennens & Lowe, 1994; Dugi *et al*., 1995; Carrière *et al*., 1997; Bezzine *et al*., 1999), guinea pig (Thomas *et al*., 2005), rat (Yang & Lowe, 2000), fungi (Holmquist *et al*., 1993; Holmquist *et al*., 1995; Brocca *et al*., 2003; Skjøt *et al*., 2009; Zhu *et al*., 2013), and bacteria (van Kampen *et al*., 1999; Santarossa *et al*., 2005; Secundo *et al*., 2006). However, these studies have been done only for lipases with one lid structure. Engineering work has not been done for any member of family I.3 lipase with two lid structures. Therefore it would be intriguing to know whether it is possible to alter the enzymatic properties of family I.3 lipase by lid engineering. If lid engineering is useful to alter the enzymatic properties of family I.3 lipase as well, this strategy can be used to increase a range of application of family I.3 lipase.

1.7. Objective of this study

The purpose of this study is to examine whether the enzymatic properties of family I.3 lipase are altered by lid engineering. PML was used as a representative member of family I.3 lipases for this purpose. A unique feature of PML and family I.3 lipase is the presence of two lids, lid1 and lid2. Because it is thought that movement of these lids from closed to open positions is responsible for interfacial activation of PML, it is expected that PML is converted from a true lipase to an esterase by deletion of these lids. However, deletion of both lid1 and lid2 may force the protein to aggregate rapidly, because a wide hydrophobic surface area, which is covered by these lids in the closed conformation, is exposed to the solvent. MD simulation for closed-to-open and open-to-closed conformational changes of PML suggests that lid2 opens after lid1 opens and lid2 is closed before lid1 is closed (Angkawidjaja *et al*., 2010). Therefore, lid2 may play a major role for interfacial activation of PML, because PML exhibits maximal activity only when lid2 is fully open upon contact with micellar substrates. Because only a part of the hydrophobic surface area of PML is exposed to the solvent by deletion of lid2, deletion of lid2 may not significantly affect the solubility of the protein. Therefore, we decided to construct the PML derivative lacking lid2 to examine whether PML is converted from a true lipase to an esterase by deletion of lid2. This study will provide a novel strategy to alter the enzymatic properties of family I.3 lipase. This study also provides a more in-depth understanding of structure and function of lid2 of family I.3 lipase.

Another unique feature of PML and family I.3 lipase is the requirement of calcium ion for activity (Amada *et al*., 2002; Meier *et al*., 2007). This calcium ion (Ca1) is catalytically essential, because it is required to anchor lid1 to the open position (Meier *et al*. 2007; Angkawidjaja *et al*., 2007; Kuwahara *et al*., 2008). As mentioned earlier, the displacement of lid1 from the closed to open conformations involve a structural rearrangement of this lid (from a helix-turn-helix structure to a long helical structure) (Fig. 1-9). This is also a unique feature of family I.3 lipase, because the conformations of lids of other lipases are not significantly changed when their positions are changed. Lid1 of PML does not assume a long α-helical structure but assumes a helix-turn-helix structure in the absence of calcium ions, probably because two aspartate residues (Asp153 and Asp157) are located close to each other when lid1 assumes a long helical structure and this structure is highly unstable due to negative charge repulsion between these two acidic residues. Therefore, I decided to construct the single mutant proteins of PML, in which Asp153 or Asp157 is replaced by Arg or Lys, to examine whether removal of Ca1 is compensated by the introduction of a salt bridge between the positions 153 and 157. This study will provide a novel strategy to create a family I.3 lipase with calcium-independent activity.

This thesis consists of four chapters. In chapter 1, the general introduction and background of this work are summarized.

In chapter 2, a lid2 deletion mutant was constructed by deleting residues 35-64 of PML. This mutant requires calcium ions for both lipase and esterase activities like PML, suggesting that it exhibits activity only when lid1 is fully open and anchored by the catalytically-essential calcium ion like PML. However, this mutant did not undergo interfacial activation. By deleting lid2, the lipase activity of PML decreased while its esterase activity increased. Model structures of this mutant in closed and open conformations were generated and optimizations with MD simulation were done. Comparison of these structures with that of PML showed that the hydrophobic surface area provided by both lids are necessary for interfacial activation of PML, since the area considerably decreased in the lid2 deletion mutant. It is proposed that lid2 is required for interfacial activation of PML. By deleting lid2, I succeeded to convert PML from a true lipase to an esterase-like enzyme.

In chapter 3, to construct a mutant with calcium-independent opening of lid1, D153 and D157 were mutated to positively-charged residues (Lys and Arg). D153R-PML is the only

mutant which exhibited lipase activity even in the absence of calcium ions. Its lipase activity was roughly half of that of PML (except for triacetin), while its esterase activity was higher than that of PML. These results indicate that D153R-PML does not require Ca1 for lid1 opening. Higher substrate concentration than CMC is necessary for interfacial activation of D153R-PML. The difference in the anchoring mechanisms of lid1 of D153R-PML and PML may account for this difference. Arg153 probably facilitates this structural change and movement of lid1 by forming a salt bridge with Asp157.

In chapter 4, general discussion of this study, summary of the novel findings and future remarks are described.

CHAPTER 2

Conversion of PML to an esterase by deletion of lid2

2.1. Introduction

Lipase and esterase differ in the presence or absence of lid. Only lipase has a lid. Because lid covers the active site of lipase in the absence of substrate and opens in the presence of substrate, lipase undergoes interfacial activation. Esterase does not undergo interfacial activation. In addition, lid in open conformation provides large hydrophobic surface, which is necessary for binding of micellar substrate. Therefore, lipase prefers micellar substrates to soluble substrates, whereas esterase prefers soluble substrates to micellar substrates.

Comparison of the closed and open conformations of PML indicates that PML has two lids, lid 1 (residues 140-167) and lid2 (residues 46-74) (Fig. 2-1). These lids cover the active site in the closed conformation, whereas they move away from the active site in the open conformation. Lid1 is sharply bent at the middle of the helix such that it assumes a helix-turn-helix structure, whereas it assumes a single long α-helix with its non-polar residues facing outward and polar residues facing inward in the open conformation. In the open conformation, lid1 is anchored by the catalytically-essential calcium ion (Ca1) to the open position (Kuwahara *et al*., 2008) and lid2 forms a helix-turn-helix structure with a preceding α-helix. Molecular dynamics (MD) simulation of PML in the open conformation in the absence of micelles and that of PML in the closed conformation in the absence of calcium ion and presence of micelles suggest that lid1 opens first and lid2 is closed first. (Angkawidjaja *et al*., 2010). This result suggests that lid2 plays a major role for interfacial activation of PML, because PML exhibits maximal activity only when lid2 fully opens. Therefore, it would be informative to examine whether PML loses an ability to undergo interfacial activation and therefore behaves as an esterase, instead of a lipase, by deletion of lid2.

In this chapter, I constructed the PML derivative lacking lid2 (ΔL2-PML) and analyzed its structure, enzymatic activity, and stability. I showed that PML becomes more similar to esterase than to lipase in enzymatic properties by deletion of lid2. I propose that deletion of lid2 is a promising strategy to convert family I.3 lipase to an esterase-like enzyme.

2.2. Materials and Methods

2.2.1. Protein preparation

The plasmid pET-25b(+) derivatives for overproduction of $\Delta L2_{all}$-PML and ΔL2-PML were constructed by amplifying the genes encoding $\Delta L2_{all}$-PML and ΔL2-PML by the PCR overlap extension method (Horton *et al*., 1990) and inserting them into the *Nde*I-*Hin*dIII sites of plasmid pET-25b(+) (Novagen Inc., Madison, WI, USA). Plasmid pET-PML for overproduction of PML (Amada *et al*., 2000) was used as a template. The 5' and 3' mutagenic primers for PCR were designed such that the DNA sequence coding for amino acids 46 to 74 (for $\Delta L2_{all}$-PML) or 35 to 64 (for ΔL2-PML) is deleted. PCR was done with 2720 Thermal Cycler (Applied Biosystems, Tokyo, Japan) using KOD+ DNA polymerase (Toyobo Co., Ltd., Kyoto, Japan) according to the procedures recommended by the supplier. PCR primers were supplied by Hokkaido System Science (Hokkaido, Japan). The DNA sequence was confirmed with ABI Prism 310 DNA sequencer (Applied Biosystems).

Overproduction of PML, $\Delta L2_{all}$-PML, and ΔL2-PML using *E. coli* HMS174(DE3)pLysS cells transformed with the pET25b(+) derivatives and purification of these proteins were carried out as described previously (Amada *et al*., 2000). The purity of the protein was analyzed by sodium dodecyl sulfate-polyacrylamide gel electrophoresis (SDS-PAGE) (Jennens & Lowe, 1994) using a 12% polyacrylamide gel, followed by staining with Coomassie Brilliant Blue R-250 (CBB). The protein concentration was determined from UV absorption on the basis that the absorbance of a 0.1% solution (1 mg/ml) at 280 nm is 1.10 for PML, 1.06 for $\Delta L2_{all}$-PML, and 1.14 for ΔL2-PML. These values were calculated by the method of Gill and von Hippel (1989).

2.2.2. Circular dichroism (CD) spectroscopy

The far-UV CD spectra were measured on a J-725 spectropolarimeter (Japan Spectroscopic Co., Ltd., Tokyo, Japan) at 20°C. The buffer used to dissolve the proteins was 5 mM Tris-HCl (pH 8) containing 5 mM $CaCl_2$ and 0.02% Triton X-100, or the same buffer containing 5 mM $CaCl_2$. The protein concentration was 0.3 mg/ml and the optical path length was 2 mm. The mean residue ellipticity (θ), which has the units of deg cm^2 $dmol^{-1}$, was calculated by using an average amino acid molecular mass of 110 Da.

2.2.3. Thermal denaturation

Thermal denaturation curves of the proteins were obtained by plotting the change in CD values at 220 nm against increasing temperature (1°C/min). The protein was dissolved either in 5 mM Tris-HCl (pH 8) containing 5 mM $CaCl_2$ and 0.02% Triton X-100, or the same buffer containing 5 mM $CaCl_2$. The protein concentration and optical path length were 0.3 mg/ml and 2 mm, respectively. The midpoint of the transition of thermal denaturation curve ($T_{1/2}$), at which 50% of the protein is denatured, was calculated from curve fitting of the resultant CD values versus temperature data on the basis of a least squares analysis.

2.2.4. Enzymatic activity

The lipase activity was determined using triacylglycerides with various chain lengths, such as triacetin (C_2), tributyrin (C_4), tricaproin (C_6), tricaprylin (C_8), and olive oil (99% triolein, C_{18}), as a substrate. The esterase activity was determined using fatty acid ethyl esters with various chain lengths, such as ethyl-butyrate (C_4), ethyl-caproate (C_6), ethyl-caprylate (C_8), ethyl-laurate (C_{12}), and ethyl-palmitate (C_{16}), as a substrate. Triglycerides with chain length from C_2 to C_8 were obtained from Sigma Chemical Co. (St Louis, MO, USA), and olive oil and fatty acid monoesters were obtained from Wako Pure Chemical Industries, Ltd. (Osaka, Japan).

For measurement of both lipase and esterase activities, appropriate amount of the enzyme was mixed with the substrate in 1.5 ml of 25 mM Tris-HCl (pH 7.5) containing 10 mM $CaCl_2$. The concentration of the substrate was 15% (v/v) (800 mM) for triacetin (C_2) and 3.7% (v/v) for other substrates. At these concentrations, all substrates form micelles, because the critical micellar concentration (CMC) of the substrate is 5.7% (v/v) (306 mM) for triacetin (C_2) and <3.7% (v/v) for other substrates. The reaction mixture was incubated at 30°C for 30 minutes with constant vigorous shaking. Reaction was terminated by the addition of 5 ml acetone-ethanol (1:1, v/v) and the amount of liberated fatty acid was titrated with 10 mM NaOH. One unit of activity is defined as the amount of enzyme that liberates 1 μmol of fatty acid per min.

2.2.5. Molecular Dynamics (MD) simulation

MD simulation was performed as described previously (Angkawidjaja *et al*., 2010). The preliminary models for the structures of ΔL2-PML in a closed and open conformation, which were constructed by deleting residues 35-64 from the crystal structures of PML in the closed (PDB ID

2Z8X) and open (PDB ID 2ZVD) conformations with the COOT program (39), respectively, were used as the initial structures.

MD simulation was done with GROMACS ver. 3.3.3 (Lindahl *et al*., 2001) on a DELL DpeR900 server (HPC Technologies Co., Tokyo, Japan) running on CentOS4. The force field used was GROMOS G53a6, with parameters supplied by GROMACS. Energy minimization and MD simulations were done in the same parameter as previously described (Angkawidjaja *et al*., 2010). MD simulation was performed for 10 ns for a closed conformation in a box of water and 7 ns for an open conformation in a box of water in the presence of micelle. The root-mean-square-deviation (RMSD) values of the Cα atoms of lid1 and the whole protein were computed with G_RMS, an auxiliary program provided with the GROMACS package. The calculation was done according to least squares fitting of the Cα atoms of trajectories during the course of simulation.

2.2.6. Structural analysis

Visualization of all of the structures shown here is made with PyMOL (The PyMOL Molecular Graphics System, Version 1.3, Schrödinger, LLC). Structural comparison of the proteins was done with the secondary structure matching (SSM) method, using the Coot program (Emsley *et al*., 201). Calculation of accessible surface area was done with AREAIMOL (Lee & Richards, 1971; Saff & Kuijlaars, 1997) within CCP4 program suite v6.1.13 (Potterton *et al*., 2003; Collaborative Computational Project, 1994).

2.3. Results

2.3.1. Mutant design

According to the crystal structures of PML in the open and closed conformations, lid2 assumes a loop-helix-loop structure (Fig. 2-1). In this structure, the first loop, α3-helix, and the second loop consist of residues 46-47, 48-58, 59-74, respectively, for open conformation (Fig. 2-2), and residues 46-49, 50-60, 61-74, respectively, for closed conformation. In order to examine whether the enzymatic properties of PML are altered by deletion of lid2, I constructed the mutant protein $\Delta L2_{all}$-PML, in which the entire lid2 region (residues 46-74) is deleted, at first. $\Delta L2_{all}$-PML was overproduced in *E. coli* in inclusion bodies, solubilized and purified in a urea-denatured form, and refolded, as was PML (Amada *et al*., 2000). The far- and near-UV CD spectra of this protein were similar to those of PML, suggesting that the overall structure of PML is not seriously changed by the deletion of lid2 (data not shown). However, it exhibited little enzymatic activity for triglyceride and fatty acid monoester substrates with various chain lengths (C_2, C_4, C_8, and C_{18} for triglycerides and C_4, C_6, C_8, C_{12}, and C_{16} for fatty acid monoesters). Because the N- and C-termini of lid2 are not located close to each other in the open conformation (Fig. 2-1B), the deletion of the entire lid2 region probably causes a local structural change, which is unfavorable for activity. Therefore, I decided to construct another mutant protein, in which residues 35-64 of PML are deleted, to minimize a conformational change caused by the deletion. The resultant mutant protein is designated as ΔL2-PML, because it lacks a large part of lid2 including α3-helix (Fig. 2-2). It lacks α2-helix as well, but retains a part of the second loop of lid2 (residues 65-74). According to the crystal structure of PML in the open conformation, α3-helix forms a helix hairpin structure with the preceding α2-helix (residues 32-43) (Fig. 2-1B). This structure exists as a relatively independent structure. In addition, residues 34 and 65 are located close to each other (Fig. 2-1B). The distance of the Cα atoms of these residues is 5.9Å, which is larger than that of the neighboring Cα atoms of polypeptide chain (typically 3.8Å), but only by 2Å. Therefore, it is expected that the deletion of residues 35-64 does not seriously affect the overall structure of PML in the open conformation. The distance of the Cα atoms of residues 34 and 65 is 11.8Å in the closed conformation, which is much larger than that in the open conformation. However, residue 65 is located in a long loop and may easily shift its position, such that it is located close to residue 34, when residues 35-64 are deleted.

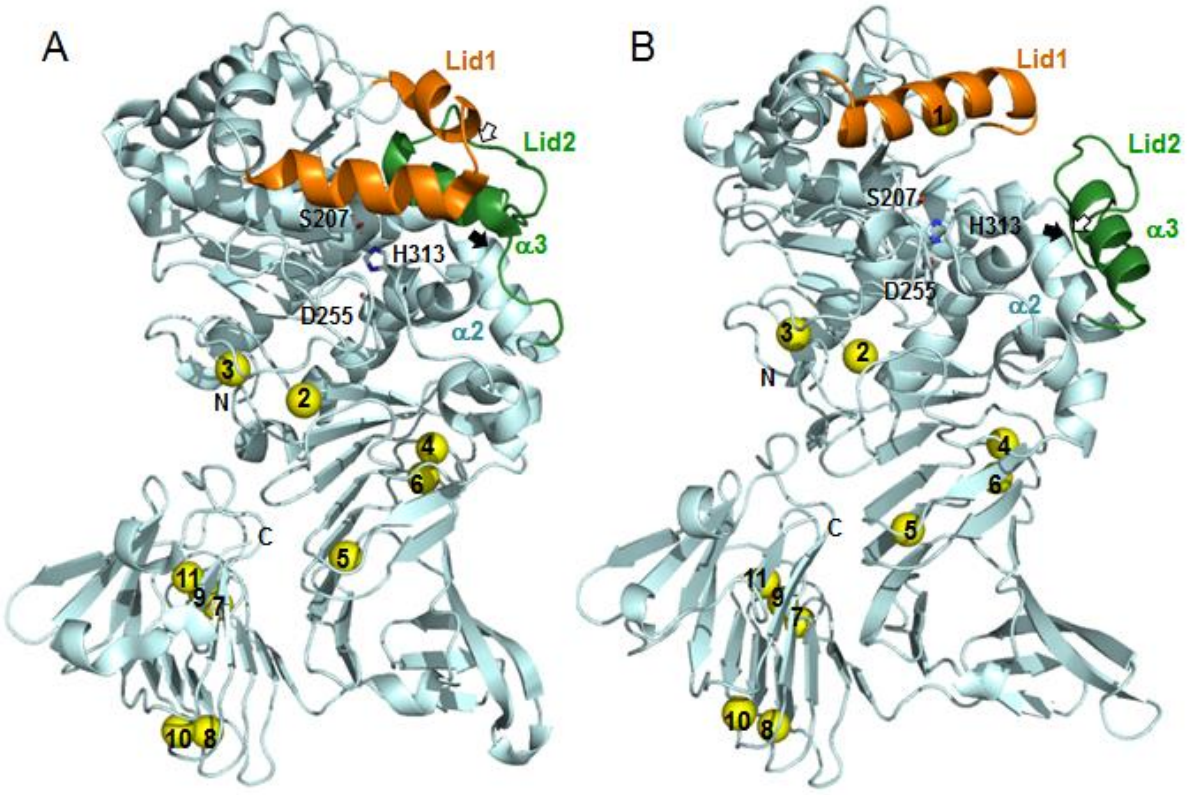

Fig. 2-1. Crystal structures of PML. The crystal structures of PML in the closed conformation (PDB ID 2Z8X) (A) and open conformation (PDB ID 2ZVD) (B) are shown. The backbone is colored cyan, lid1 is colored orange, and lid2 is colored green. Eleven calcium ions are shown as yellow spheres with their numbers indicated. Three active site residues (Ser207, Asp255, His313) are indicated by stick models, in which the oxygen atoms are colored red and the nitrogen atoms are colored blue. The solid and open arrows indicate the N-terminal (Gly35) and C-terminal (Gln64) residues of the sequence deleted in ΔL2-PML, respectively. N- and C, N- and C-terminus, respectively.

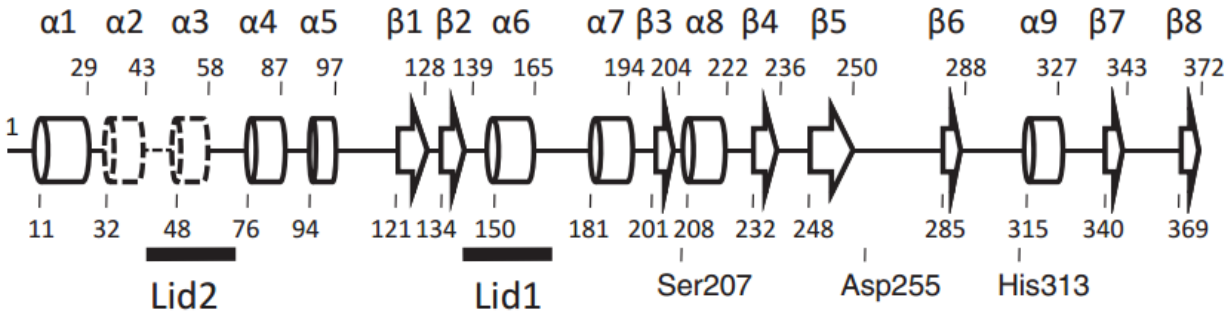

Fig. 2-2. Schematic representation of primary structure of PML. The primary structure of the N-domain (residues 1-372) of PML is schematically shown. The α-helices and β-strands are represented by cylinders and arrows, respectively. These secondary structures are arranged based on the crystal structure of PML in the open conformation. Numbers indicate the positions of the residues relative to the initiator methionine residue of the protein. The ranges of lid1 and lid2, and the positions of three active-site residues (Ser207, Asp245, His313) are also shown. The region containing α2- and α3-helices, which is deleted in ΔL2-PML, is indicated by broken lines.

2.3.2. Biochemical properties

ΔL2-PML was overproduced in *E. coli* as inclusion bodies, solubilized and purified in a urea-denatured form, and refolded in the presence of calcium ions, as was PML (Amada *et al*., 2000). The production level of ΔL2-PML was similar to that of PML (Fig. 2-3). The amount of the protein purified from one liter culture was typically 20-30 mg, which is comparable to that of PML. The molecular mass of ΔL2-PML estimated from gel filtration chromatography (68 kDa) is comparable to the calculated one (61,597 kDa), suggesting that it exists as a monomer as does PML.

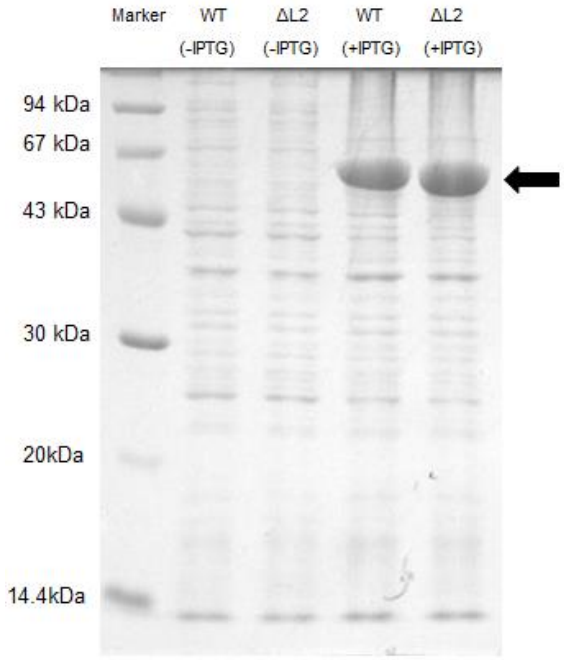

Fig. 2-3. Comparison of the production levels of PML and ΔL2-PML by SDS-PAGE.

PML assumes the closed conformation in the presence of 5 mM $CaCl_2$ and absence of micellar substances, while it assumes the open conformation in the presence of 5 mM $CaCl_2$ and 0.02% Triton X-100, as revealed by the crystal structures of PML (11). The far-UV CD spectra of ΔL2-PML and PML were measured either in the presence of 5 mM $CaCl_2$ and absence of Triton X-100, or in the presence of 5 mM $CaCl_2$ and 0.02% Triton X-100. The former spectra are shown in Figure 2-4. The latter spectra are not shown, because the spectrum of ΔL2-PML or PML determined in the absence of Triton X-100 was nearly identical to that determined in the presence of Triton X-100. The far-UV CD spectrum of ΔL2-PML is nearly identical to that of PML (Fig. 2-

4), suggesting that there is no significant difference in the overall structure between ΔL2-PML and PML, both in the closed and open conformations.

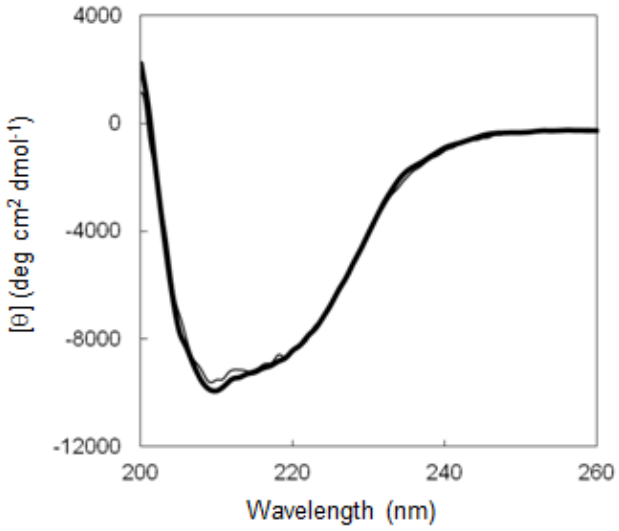

Fig. 2-4. Far-UV CD spectra. The far-UV CD spectra of PML (thick line) and ΔL2-PML (thin line) were measured at 20°C in 5 mM Tris-HCl (pH 8) containing 5 mM $CaCl_2$ as described under Materials and Methods.

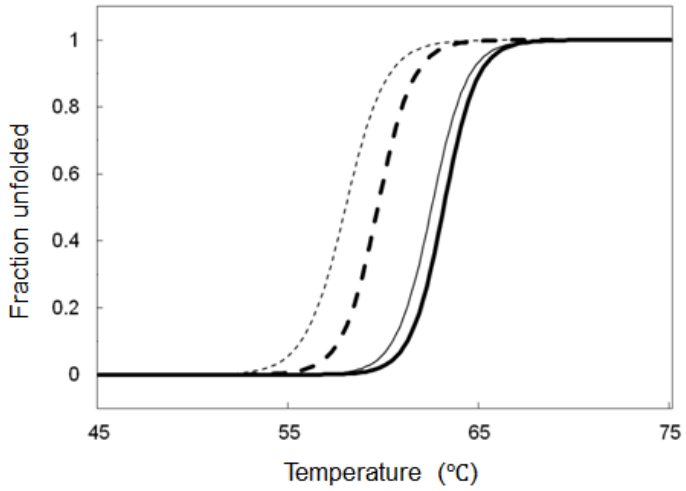

Fig. 2-5. Thermal denaturation curves. The thermal denaturation curves of PML measured either in the absence of Triton X-100 (thick line) or presence of 0.02% Triton X-100 (thick broken line), and ΔL2-PML measured either in the absence of Triton X-100 (thin line) or presence of 0.02% Triton X-100 (thin broken line) are shown. The curves were recorded by monitoring the change in CD values at 220 nm as described under Materials and Methods.

To examine whether the deletion of residues 35-64 affects the stability of PML, thermal denaturation of ΔL2-PML and PML was analyzed either in the presence of 5 mM $CaCl_2$ and absence of Triton X-100, or in the presence of 5 mM $CaCl_2$ and 0.02% Triton X-100, by

monitoring the change in CD values at 220 nm as the temperature increased. The results are shown in Figure 2-5. The midpoint of the transition of the thermal denaturation curve, $T_{1/2}$, was 59.6°C for ΔL2-PML and 63.1°C for PML in the absence of Triton X-100, and 57.9°C for ΔL2-PML and 62.5°C for PML in the presence of Triton X-100. These results indicate that lid2 contributes to the stabilization of PML by 4-5°C, regardless of whether it assumes the open or closed conformation.

2.3.3. Enzymatic activity

The enzymatic activities of PML and ΔL2-PML were determined by using various triglycerides and fatty acid ethyl esters with different acyl chain lengths as a substrate at pH 7.5 and 30°C in the presence of 10 mM $CaCl_2$. PML showed wide preference for triglycerides with the highest preference for tributyrin (C_4) among various triglyceride substrates examined (Fig. 2-6A). This result is consistent with that previously reported (Amada *et al*., 2000). ΔL2-PML showed similar preference for triglycerides as that of PML, but exhibited lower activities than those of PML especially for long acyl chain substrates, such as tricaprylin (C_8) and olive oil (C_{18}) (Fig. 2-6A). The activities of ΔL2-PML toward tributyrin (C_4) and olive oil (C_{18}) were 70 and 21% of those of PML, respectively. In contrast, ΔL2-PML exhibited higher activities than those of PML for all fatty acid ethyl esters examined (Fig. 2-6B). The preference of ΔL2-PML for various fatty acid ethyl esters was slightly different from that of PML. However, both enzymes showed the highest preference to ethyl-caproate (C_6). The activity of ΔL2-PML toward this substrate was 1.6-fold higher than that of PML. The optimum temperature for activity of ΔL2-PML (45°C), which was measured using triacetin (C_2) as a substrate at the substrate concentration of 1 M, was comparable to that of PML, suggesting that the difference in the stability between ΔL2-PML and PML is too small to affect the optimum temperature for activity.

PML requires calcium ion for activity, because anchoring of lid1 by the calcium ion (Ca1) is crucial to stabilize the open conformation of lid1 (Angkawidjaja *et al*., 2010). To examine whether ΔL2-PML also requires calcium ion for activity, the enzymatic activity of ΔL2-PML was determined in the absence of calcium ions. Tributyrin (C_4) and ethyl-caproate (C_6) were used as a substrate. ΔL2-PML exhibited little activity for these substrates in the absence of calcium ions as does PML, indicating that ΔL2-PML requires calcium ion for activity. Anchoring of lid1 by Ca1

to stabilize its open conformation is probably necessary for enzymatic activity of ΔL2-PML as well.

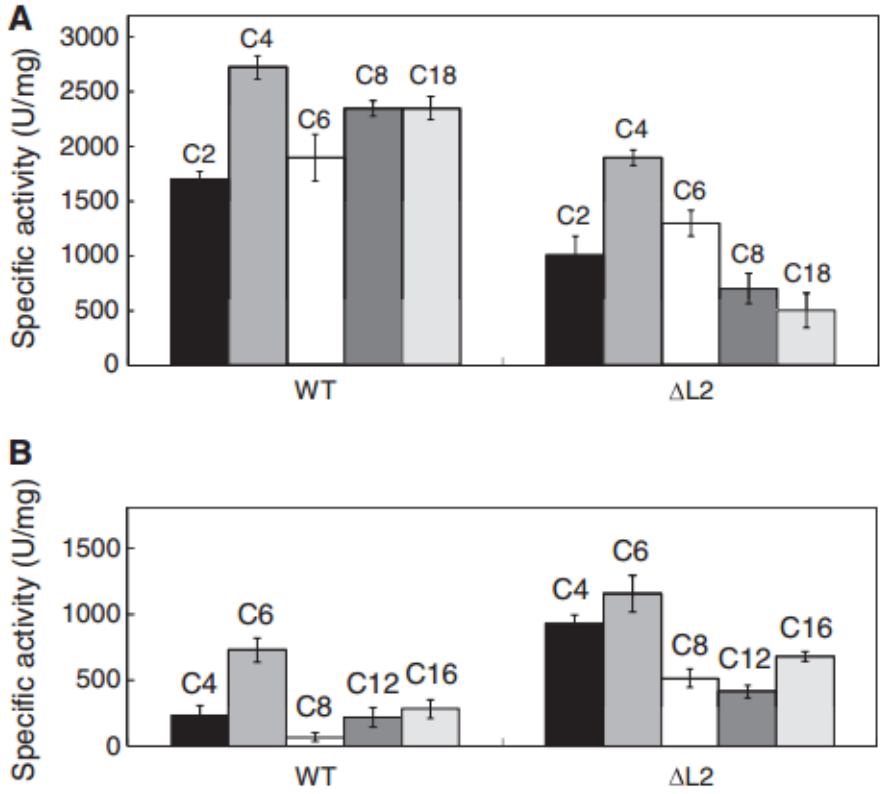

Fig. 2-6. Substrate selectivity of PML and ΔL2-PML. Specific activities of PML (WT) and ΔL2-PML (ΔL2) toward triglyceride substrates (A) and fatty acid monoester substrates (B) are shown. C2~C18 represent the acyl chain lengths of the substrates. The experiment was carried out in duplicate. Each value represents the average value and errors from the average values are shown.

2.3.4. Interfacial activation

To examine whether the interfacial activation of PML is altered by deletion of lid2, the activity of ΔL2-PML was determined at different concentrations of triacetin (C_2). The activity of PML was also determined in the same condition for comparative purpose. The results are shown in Figure 2-7. As reported previously (Amada *et al.*, 2000), the PML activity significantly increased when the substrate concentration reached and increased beyond the critical micellar concentration (CMC) (306 mM). As a result, the plot of PML activity as a function of the triacetin (C_2) concentration has a sigmoidal shape. In contrast, this plot has a hyperbolic shape for ΔL2-PML, indicating that ΔL2-PML does not undergo interfacial activation. This result showed that

deletion of lid2 altered the property of PML, and that lid2 is required for interfacial activation of PML.

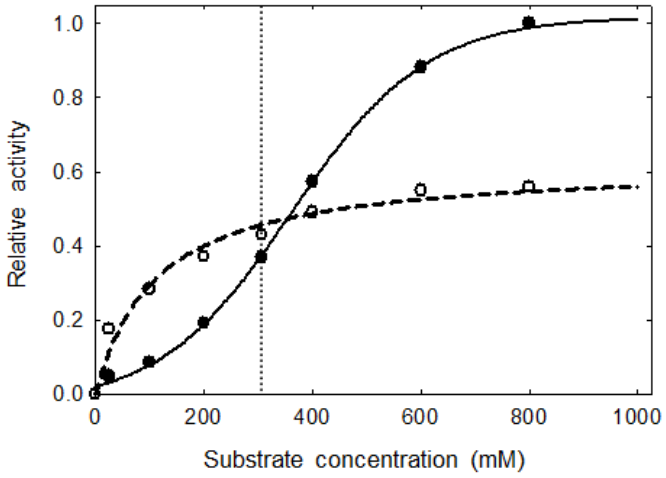

Fig. 2-7. Dependencies of the PML and ΔL2-PML activities on the concentration of triacetin. The enzymatic activities of PML (closed circle) and ΔL2-PML (open circle) relative to those determined in the presence of 800 mM triacetin are shown as a function of the triacetin concentration. A vertical dotted line represents the CMC of triacetin, which is 306 mM. The experiment was carried out in duplicate and the errors were within 10% of the values reported.

2.3.5. MD simulation of ΔL2-PML structure

To construct models for three-dimensional structures of ΔL2-PML in a closed and open conformation, MD simulation was performed. The structures constructed by simply deleting residues 34-65 from the crystal structures of PML in the closed and open conformations were used as the initial structures. The average RMSD value of the Cα atoms of ΔL2-PML in the closed conformation between the initial and simulated structures gradually increases in the beginning and becomes nearly constant in the end during simulation (Fig. 2-8A). This change is more significant for lid1 than for the entire protein, suggesting that lid1 moves much more significantly than does the entire protein. The difference in the positions of lid1 in the closed conformation before and after MD simulation is shown in Figures 2-9A and 2-9B. Lid1 changes its position after MD simulation, such that lid1 contacts the remaining lid2 loop (residues 65-74) and covers the hydrophobic catalytic pocket, due to hydrophobic collapse. During the early course of simulation, lid1 probably moves deeper towards the catalytic pocket to increase hydrophobic interactions between lid1 and the catalytic pocket. The accessible surface area (ASA) of the O^{γ} atom of the active site serine residue (Ser207 O^{γ}) is calculated to be 0.3Å^2 for PML, 13.1Å^2 for ΔL2-PML

before MD simulation, and 1.5Å^2 for ΔL2-PML after MD simulation (percent exposure of 0.6, 24.8, and 2.8%, respectively). Thus, the catalytic pocket of ΔL2-PML is more likely inaccessible from the solvent in the closed conformation. All other parts of the protein that move during simulation are loops, including the remaining lid2 loop. Movement of the loop structure is common in MD simulation, because loops are mostly flexible.

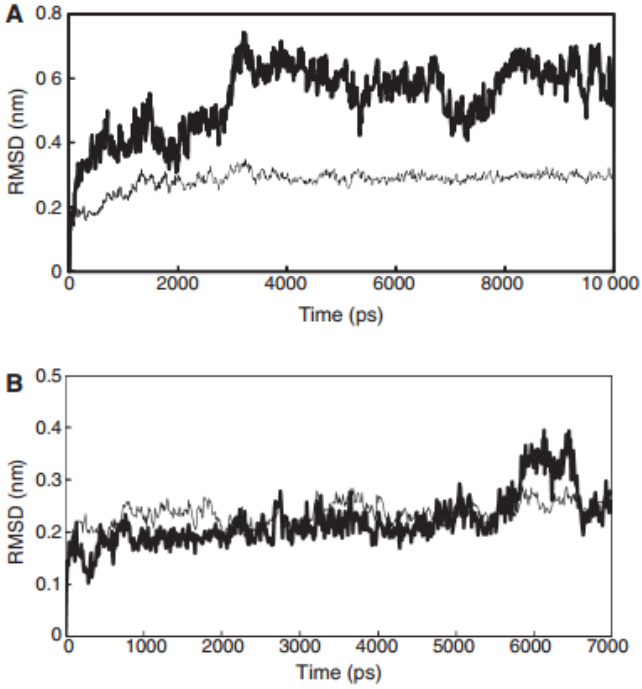

Fig. 2-8. The RMSD between the initial and simulated structures of ΔL2-PML. The RMSD between the initial and simulated structures of ΔL2-PML in a closed (A) and open (B) conformation following a least squares fit using the backbone atoms as a reference are shown as a function of the simulation time. The open conformation of ΔL2-PML is simulated in the presence of octane. The RMSD values of the regions corresponding to lid1 and the entire protein are shown by thick and thin lines, respectively.

The average RMSD value of the Cα atoms of lid1 in the open conformation between the initial and simulated structures is nearly constant and is similar to that of the entire protein during simulation (Fig. 2-8B). There is a jump in the RMSD value of lid1 Cα atoms at around 6 ns. However, this jump did not last long and the RMSD value went down at around 6.6 ns. Furthermore, comparison of the open conformation structures of ΔL2-PML before and after MD simulation with octane micelle shows only slight movement of lid1 (Fig. 2-9C). These results suggest that there is no significant change in the overall structure of ΔL2-PML in the open conformation, which is highly similar to that of PML, before and after MD simulation. It is noted that the remaining lid2 loop changes its position after MD simulation, such that it is located at the

position where the deleted region of lid2 is located (lower middle panel of Fig. 2-9A and Fig. 2-9C). This loop changes its position probably because it is highly flexible.

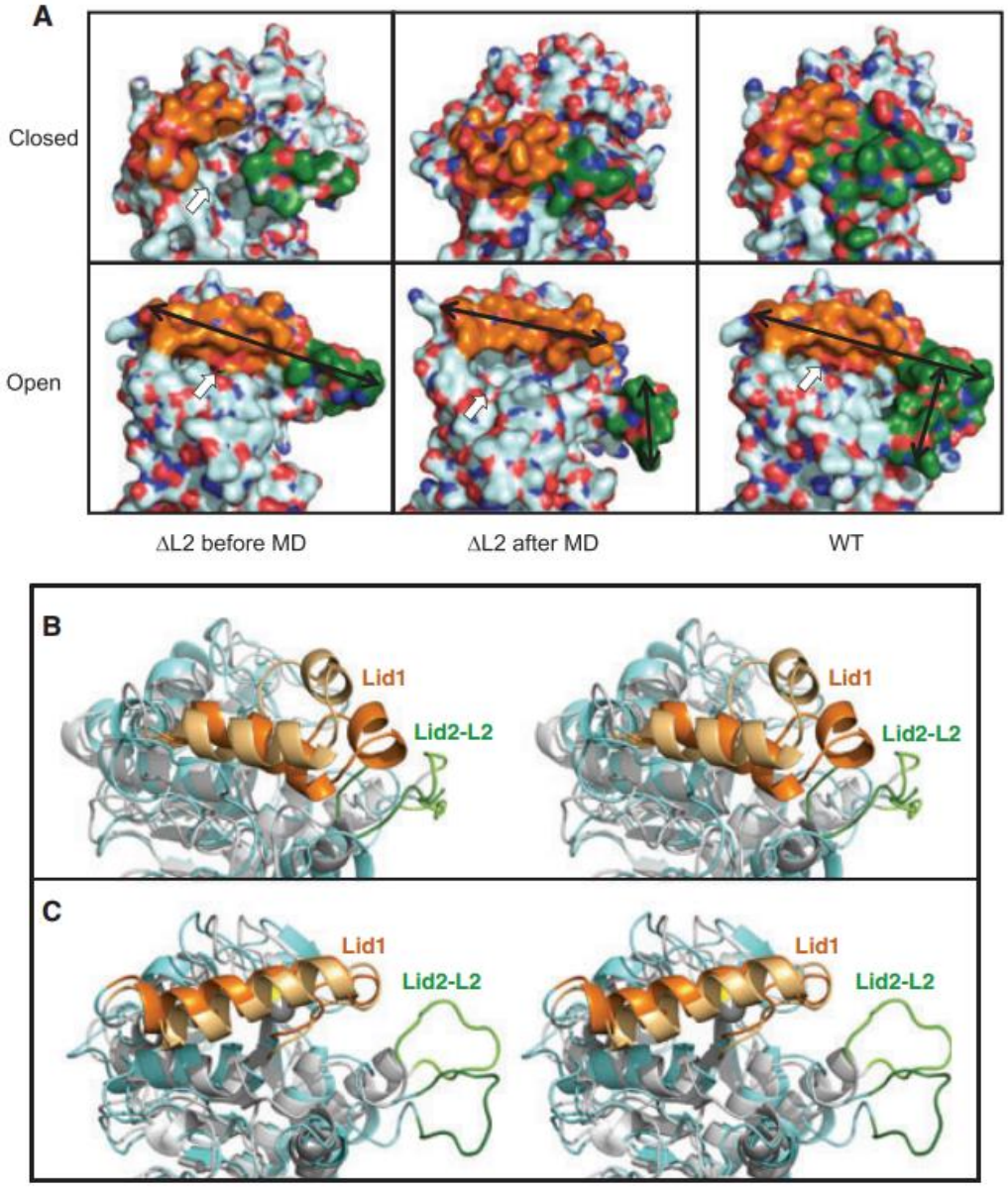

Fig. 2-9. Comparison of the initial and simulated structures of ΔL2-PML around the active site. (A) Surface representations of the initial (before MD, left column) and simulated (after MD, middle column) structures of ΔL2-PML, in a closed (upper row) and open (lower row) conformation, are shown in comparison with those of the crystal structures of PML (right column). The backbone is colored cyan, lid1 is colored orange, and lid2 is colored green. The nitrogen and oxygen atoms are colored blue and red, respectively. Open arrow points to the exposed catalytic pocket in a closed conformation. Double-headed arrow shows the range of the hydrophobic surface provided by lid(s) in an open conformation. (B, C) Stereo views of the ΔL2-PML structures in a closed (B) and open (C) conformation. The simulated structure, in which the backbone is colored cyan, lid1 is colored orange, and the remaining lid2 loop is colored green, is superimposed onto the initial structure, in which the backbone is colored grey, lid1 is colored light orange, and the remaining lid2 loop is colored light green.

2.4. Discussion

2.4.1. Validity of simulated structure of ΔL2-PML

Validity of the simulated structure of ΔL2-PML is discussed below for closed and open conformations separately. For the closed conformation, the simulated structure is different from the initial structure, which is constructed by simply deleting residues 35-64 from the crystal structure of PML in the closed conformation, mainly in the position of lid1. Lid1 does not fully cover the hydrophobic catalytic pocket of ΔL2-PML in the initial structure, while it almost fully covers it in the simulated structure (Figs. 2-9A, B). The observation that ΔL2-PML exhibits little activity in the absence of calcium ions even for ethyl-caproate (C_6) suggests that the catalytic pocket of ΔL2-PML is not solvent-exposed but is covered by lid1. If the catalytic pocket of ΔL2-PML is partially solvent-exposed, ΔL2-PML would permit this substrate to access its catalytic pocket and therefore exhibit at least slight activity for this substrate even in the absence of calcium ions. Opening of lid1 and stabilization of the open conformation of lid1 by Ca1 are probably required for the activation of ΔL2-PML, as reported for PML (Angkawidjaja *et al*., 2010). Coverage of the hydrophobic pocket of ΔL2-PML by lid1 may also be supported by the observation that ΔL2-PML exists as a monomer in aqueous solution. Proteins are prone to aggregate when their interior hydrophobic regions are exposed to the solvent. Thus, the simulated structure of ΔL2-PML is apparently more valid than its initial structure.

For the open conformation, the simulated structure is similar to the initial structure, which is constructed by simply deleting residues 35-64 from the crystal structure of PML in the open conformation, except for the position of the remaining lid2 loop. This result suggests that the deletion of lid2 does not cause instability of the open conformation of lid1. The remaining lid2 loop contacts lid1 in the initial structure (lower left panel of Fig. 2-9A, Fig. 2-9C), but does not contact it in the simulated structure (lower middle panel of Fig. 2-9A, Fig. 2-9C). The shift in the position of this loop is probably caused by a strong hydrophobic interaction with a micelle. Because the position of this loop in the simulated structure is apparently more suitable for binding of micellar substrates than that in the initial structure and ΔL2-PML retains substantial level of activities for triglyceride substrates, the simulated structure may be more valid than the initial structure. Attempts to determine the crystal structures of ΔL2-PML both in the closed and open conformations have so far been unsuccessful.

2.4.2. Effect of lid2 deletion on enzymatic activity of PML

In the closed conformation of PML, both lid1 and lid2 assume amphiphilic α-helical structures with hydrophobic surfaces facing inward to the protein core and hydrophilic surfaces facing outward. Upon contact with a micellar substrate, these lids change conformation, and the orientations of their hydrophobic surfaces are flipped, providing a wide continuous hydrophobic surface spanning from lid1 to lid2, to bind to the substrate (Fig. 2-9A, lower right panel). With deletion of the most part of lid2, a relatively large hydrophobic surface is lost, and the once continuous hydrophobic surface becomes discontinuous by the loss of contact between lid1 and the remaining loop of lid2 (Fig. 2-9A, lower middle panel). Wide hydrophobic surface provided by both lid1 and lid2 may be required for optimal binding of PML to substrate, which leads to optimal catalytic activity. The activities of ΔL2-PML toward all the triglyceride substrates examined, especially those toward substrates with longer acyl chains (C_8 and C_{18}), decrease as compared to those of PML, probably because the capability of PML to bind effectively to substrate decreases, due to the loss of hydrophobic surface provided by lid2.

In contrast, the activities of ΔL2-PML toward all the fatty acid monoester substrates examined increase as compared to those of PML. This result suggests that these substrates can access the catalytic pocket of ΔL2-PML more readily than that of PML. Fatty acid monoester substrates are less hydrophobic and more water-soluble than triglyceride substrates. These substrates exist as monomers or as small aggregates, known as pre-micelles (Hadgiivanova *et al*., 2007; Cui *et al*., 2008). Therefore, it is highly likely that contact with these substrates is sufficient for the opening of lid1 and stabilization of the open conformation of lid1 by Ca1 is sufficient for the activation of both PML and ΔL2-PML. However, contact with these substrates may not be sufficient for opening of lid2. In fact, MD simulation suggests that the opening of lid2 is triggered by that of lid1 and the open conformation of lid2 is intrinsically unstable (Angkawidjaja *et al*., 2010). Thus, PML is less active than ΔL2-PML toward fatty acid monoester substrates, probably because lid2 limits the accessibility of these substrates to the catalytic pocket of PML. Deletion of lid2 had successfully altered the substrate preference of PML from the bulky triglycerides to fatty acid monoester substrates.

Since interfacial activation was lost in ΔL2-PML, it is clear that by deleting lid2 from PML, the enzymatic property of PML was altered from that of a true lipase to become more similar to esterase. As mentioned above, lid1 may open regardless of whether it contacts a micellar or non-

micellar substrate, but its hydrophobic surface in the open conformation may not be sufficient for effective binding to a micellar substrate. Wide and continuous hydrophobic surface provided by both lid1 and lid2 may be required for stable and firm binding of a micellar substrate to the catalytic pocket and therefore for maximal activity. However, lid2 may fully and stably open to permit the maximal accessibility of a substrate to the catalytic pocket, only when it contacts a micellar substrate. This is the reason why the enzymatic activity of PML significantly increases when the substrate concentration reaches CMC and increases beyond. I propose that the presence of a micellar substrate is necessary to promote full opening of lid2, and the hydrophobic surface provided by lid2 is necessary for a stable and firm binding of a micellar substrate to the catalytic pocket.

Lipase is distinguished from esterase in its ability to catalyze long-chain triglycerides (Nardini & Dijkstra, 1999), and esterase is distinguished from lipase in its ability to catalyze more soluble substrates (Fojan *et al*., 2000). Lipase undergoes interfacial activation, while esterase does not. Because ΔL2-PML exhibits comparable activities toward long-chain triglycerides and short-chain fatty acid monoesters (Fig. 2-6), and does not undergo interfacial activation, it is not defined as a true lipase but is defined as an intermediate between lipase and esterase. Thus, lid2 is required to give an ability to PML to function as a true lipase. By using PML as an example, deletion of lid2 can be applied as one of the engineering approaches to alter the function of other family I.3 lipase as well. PML loses activity by the deletion of the entire lid2 region, probably due to a configurational perturbation around the active site. However, a possibility that a part of the second loop of lid2 (residues 65-74), which is not deleted in ΔL2-PML, is required for activity cannot be excluded.

The role of lid has been extensively studied using lipases from human (Jennens & Lowe, 1994; Dugi *et al*., 1995; Carrière *et al*., 1997; Bezzine *et al*., 1999), guinea pig (Thomas *et al*., 2005), rat (Yang & Lowe, 2000), fungi (Holmquist *et al*., 1993; Holmquist *et al*., 1995; Brocca *et al*., 2003; Skjøt *et al*., 2009; Zhu *et al*., 2013), and bacteria (van Kampen *et al*., 1999; Santarossa *et al*., 2005; Secundo *et al*., 2006). These studies indicate that lid is important for activity and substrate selectivity of lipase, and showed that mutation in lid structure can alter the property of lipase. However, all studies have been done for lipases with only single lids. Therefore this is the first report on the alteration of enzymatic properties of a lipase with two lid structures by lid engineering.

2.5. Summary

A family I.3 lipase from *Pseudomonas* sp. MIS38 (PML) is characterized by the presence of two lids (lid1 and lid2) that greatly change conformation upon substrate binding. To examine whether PML is converted from a true lipase to an esterase by deletion of lid2, a lid2 deletion mutant (ΔL2-PML) was constructed by deleting residues 35-64 of PML. ΔL2-PML requires calcium ions for both lipase and esterase activities as does PML, suggesting that it exhibits activity only when lid1 is fully open and anchored by the catalytically-essential calcium ion as does PML. However, when the enzymatic activity was determined using triacetin, the activity of PML exponentially increased as the substrate concentration reached and increased beyond the critical micellar concentration (CMC), while that of ΔL2-PML did not. These results indicate that PML undergoes interfacial activation, while ΔL2-PML does not. The activities of ΔL2-PML for long-chain triglycerides significantly decreased while its activity for fatty acid ethyl esters increased, as compared to those of PML. Comparison of the tertiary models of ΔL2-PML in a closed and open conformation, which are optimized by MD simulation, with the crystal structures of PML suggests that hydrophobic surface area provided by lid1 and lid2 in an open conformation is considerably decreased by the deletion of lid2. I propose that hydrophobic surface area provided by these lids is necessary to hold the micellar substrates firmly to the active site and therefore lid2 is required for interfacial activation of PML. By deleting lid2, I succeeded in altering the properties of PML from that of a true lipase to more of an esterase.

CHAPTER 3

Creation of PML with calcium-independent activity by single mutation at lid1

3.1. Introduction

Calcium ions are important for structure, stability, and/or activity of various lipases (Svendsen *et al*., 1995; Talon *et al*., 1995; Kim *et al*., 1997; Oh *et al*., 1999; Simons *et al*., 1999; Yang *et al*., 2000; Tanaka *et al*., 2003; Papaleo & Invernizzi, 2011). They are important for folding, stability, and activity of PML as well (Amada *et al*., 2001; Angkawidjaja *et al*., 2005, 2007; Kuwahara *et al*., 2008). Ten and eleven calcium ions bind to PML in the closed and open conformations, respectively (Angkawidjaja *et al*., 2007, 2010). The number of calcium ions bound to the closed conformation of PML is lower than that bound to the open conformation of PML by one, because Ca1 only binds to the open conformation. In addition to Ca1, Ca2 and Ca3 bind to the N-domain of PML, both of which are important for stability (Kuwahara *et al*., 2008). The rest of the calcium ions (Ca4-Ca11) bind to the C-domain of PML. These calcium ions are required for folding of a β-roll sandwich structure (Angkawidjaja *et al*., 2007). Comparison of the amino acid sequences of family I.3 lipases (Angkawidjaja & Kanaya, 2006), determination of the crystal structure of SML (Meier *et al*., 2007), modeling of the 3D structure of *Pseudomonas* sp. AMS8 lipase (Mohamad Ali *et al*., 2013), and characterization of *Pseudomonas* sp. CR-611 lipase (Panizza *et al*., 2013) suggest that other members of family I.3 lipase also have the similar/same calcium ions with similar/same roles as those of PML.

PML requires calcium ion for activity, because it requires single calcium ion (Ca1) to anchor lid1 to the open position (Fig. 3-1B,C). Contact with micellar substrates alone is not sufficient for full opening of lid1 and interfacial activation (Angkawidjaja *et al*., 2010). This calcium-dependent opening of lid1 is probably a characteristic common to family I.3 lipases (Meier *et al*., 2007; Mohamad Ali *et al*., 2013; Panizza *et al*., 2013). Ca1 of PML is hexacoordinated with the side chains of Gln120, Asp153 (monodentate), and Asp157 (bidentate), and the main chain oxygen atoms of Thr118 and Ser144 (Fig. 3-1C). Asp153 and Asp157, which are the only acidic residues at the Ca1 site and are located in lid1, are located far away from each other when lid1 is sharply bent in the closed conformation. These residues are located closer to

each other when lid1 assumes a long helix in the open conformation. The shortest distance between the $O^{\delta 1}$ or $O^{\delta 2}$ atom of Asp153 and that of Asp157 is 5.6Å in the closed conformation and 3.4Å in the open conformation. Lid1 may not assume a long helix unless Asp153 and Asp157 coordinate with Ca1, because these residues may not be able to come close to each other due to negative charge repulsion. Therefore, it would be informative to examine whether lid1 opens in a calcium-independent manner by mutating Asp153 or Asp157 to a positively charged residue.

As mentioned above, PML requires Ca4-Ca11 for folding of a β-roll sandwich. Because these calcium ions, except for Ca6 and Ca10, bind to the protein too tightly to be removed by dialysis against calcium-free buffer, PML is kept folded even when it is dialyzed against calcium-free buffer (Amada *et al*., 2001; Angkawidjaja *et al*., 2010). Nevertheless, this protein, which has previously been termed Holo-PML* (Amada *et al*., 2001), does not exhibit activity in the absence of calcium ions, because it requires Ca1 for activity. In this study, PML derivatives that require and do not require Ca1 for their activity will be designated as PML derivatives with calcium-dependent and calcium-independent activities, respectively. Even a PML derivative with calcium-independent activity requires calcium ions for folding of the C-domain (β-roll sandwich).

In this study, I constructed D153K-, D153R-, D153A-, D157K-, D157R-, D153A/D157A-, and D153R/D157N-PMLs and examined their lipase and esterase activities. D157A-PML has previously been shown to be inactive even in the presence of calcium ions (Kuwahara *et al*., 2008). Only D153R-PML exhibited both lipase and esterase activities in the absence of calcium ions, although its lipase activity was lower than that of PML by 7 fold. Because other mutants did not exhibit activity either in the presence or absence of calcium ions, lid1 of D153R-PML probably opens in a calcium-independent manner due to electrostatic attraction between Arg153 and Asp157. I propose that mutation of a negatively-charged residue to a positively-charged one at the Ca1 site is a promising strategy to create family I.3 lipase with calcium-independent activity.

3.2. Materials and Methods

3.2.1. Mutagenesis

The pUC18 derivatives for secretion of D153K-PML, D153R-PML, D153A-PML, D157K-PML, D157R-PML, D153A/D157A-PML, and D153R/D157N-PML were constructed using KOD mutagenesis kit (Toyobo) according to the supplier's instructions. Plasmid pUC-PML for secretion of PML (Kwon *et al*., 2002) was used as a template. The mutagenic primers were designed such that the codon for Asp153 (GAT) is changed to AAG for Lys, AGG for Arg, and GCT for Ala, and the codon for Asp157 (GAC) is changed to AAG for Lys, CGC for Arg, GCC for Ala, and AAC for Asn. The pUC18 derivative for secretion of D157A-PML was previously constructed (Kuwahara *et al.*, 2008). PCR was performed with 2720 Thermal Cycler (Applied Biosystems). All primers were purchased from Hokkaido System Science. The DNA sequence were confirmed with an ABI Prism 310 DNA sequencer (Applied Biosystems).

3.2.2. Secretion and purification

All PML mutants were secreted into the external medium using *E. coli* DH5 cells transformed with plasmid pYBCD20 harboring the *lipBCD* gene encoding a T1SS (Lip system) from *S. marcescens* and the pUC18 derivatives harboring the genes encoding the PML mutants, as described previously (Kuwahara *et al.*, 2008). The secreted proteins were purified as described previously (Kwon *et al*., 2002), with slight modifications. The protein was precipitated from the culture supernatant by 80% saturated ammonium sulfate, dissolved in 50 mM Tris-HCl (pH 8) containing 5% (v/v) glycerol and 10 mM $CaCl_2$, and dialyzed against the same buffer. The protein solution was concentrated by Amicon concentrator (Milipore) using a 30 kDa cut-off membrane and subjected to size exclusion chromatography using a HiLoad 16/60 Superdex 200 column (GE Healthcare) equilibrated with 5 mM Tris-HCl (pH 8). The purity of the protein was analyzed by sodium dodecyl sulfate-polyacrylamide gel electrophoresis (SDS-PAGE) (Jennens & Lowe, 1994) using a 12% polyacrylamide gel, followed by staining with Coomassie Brilliant Blue R-250 (CBB). The protein concentration was determined from UV absorption on the basis that the absorbance of a 0.1% solution (1 mg/ml) at 280 nm is 1.1 for PML and its derivatives. These values were calculated by the method of Gill and von Hippel (1989).

3.2.3. Circular dichroism (CD) spectroscopy

The CD spectra were measured on a J-725 spectropolarimeter (Japan Spectroscopic) at 20°C. The protein was dissolved in 5 mM Tris-HCl (pH 8) containing 5 mM $CaCl_2$. The protein concentration and optical path length were 0.1 mg/ml and 2 mm for far-UV CD spectra, and 0.5 mg/ml and 10 mm for near-UV CD spectra, respectively. The mean residue ellipticity (θ), which has the units of deg cm^2 $dmol^{-1}$, was calculated by using an average amino acid molecular mass of 110 Da.

3.2.4. Enzymatic activity

Lipase activity was determined by using triglycerides with various chain lengths, such as triacetin (C2), tributyrin (C4), tricaproin (C6), tricaprylin (C8), triolein (C18), olive oil, as substrates. Esterase activity was determined using fatty acid ethyl esters with various chain lengths, such as ethyl-butyrate (C4), ethyl-caproate (C6), ethyl-caprylate (C8), ethyl-laurate (C12), and ethyl-palmitate (C16), as substrates. Triglycerides with chain lengths from C4 to C8 were obtained from Sigma-Aldrich. Triglycerides with chain lengths of C2 and C18, olive oil, and fatty acid ethyl esters were obtained from Wako Pure Chemical.

For measurement of both lipase and esterase activities, appropriate amount of the enzyme was mixed with the substrate in 1.5 ml of 25 mM Tris-HCl (pH 7.5) or the same buffer containing 10 mM $CaCl_2$. The concentration of the substrate was 15% (v/v) (800 mM) for triacetin (C2) and 3.7% (v/v) for other substrates. At these concentrations, all lipase substrates form micelles, because the critical micellar concentration (CMC) is 5.7% (v/v) (306 mM) for triacetin (C2) and <3.7% (v/v) for other lipase substrates. The reaction mixture was incubated at 30°C for 30 minutes with constant vigorous shaking. Reaction was terminated by the addition of 5 ml acetone-ethanol (1:1, v/v) and the amount of liberated fatty acid was titrated with 10 mM NaOH. One unit of activity is defined as the amount of enzyme that liberates 1 μmol of fatty acid per min.

3.2.5. Thermal denaturation

The thermal denaturation curves of the proteins were obtained by plotting the change in CD values at 220 nm against increasing temperature (1°C/min). The protein was dissolved in 5 mM Tris-HCl (pH 8), the same buffer containing 5 mM $CaCl_2$, the same buffer containing 0.02% Triton X-100, or the same buffer containing both 5 mM $CaCl_2$ and 0.02% Triton X-100. The protein concentration and optical path length were 0.2 mg/ml and 2 mm, respectively. The midpoint of the transition of thermal denaturation curve ($T_{1/2}$), at which 50% of the protein is denatured, was calculated from curve fitting of the resultant CD values versus temperature data.

3.3. Results

3.3.1. Mutant preparation

To examine whether lid1 is open in the absence of calcium ions by the mutation of Asp153 or Asp157 to a positively charged residue (Lys or Arg), D153K-, D153R-, D157K, and D157R-PMLs were constructed. It had been shown previously that D157A-PML with the mutation of Asp157 to Ala is inactive either in the presence or absence of calcium ions (Kuwahara *et al*., 2008). To confirm that elimination of a negative charge repulsion between Asp153 and Asp157 is not sufficient for calcium-independent opening of lid1, D153A-PML with the mutation of Asp153 to Ala, D153A/D157A-PML with the double mutations of Asp153 and Asp157 to Ala, and D153R/D157N-PML with the double mutations of Asp153 to Arg and Asp157 to Asn were also constructed.

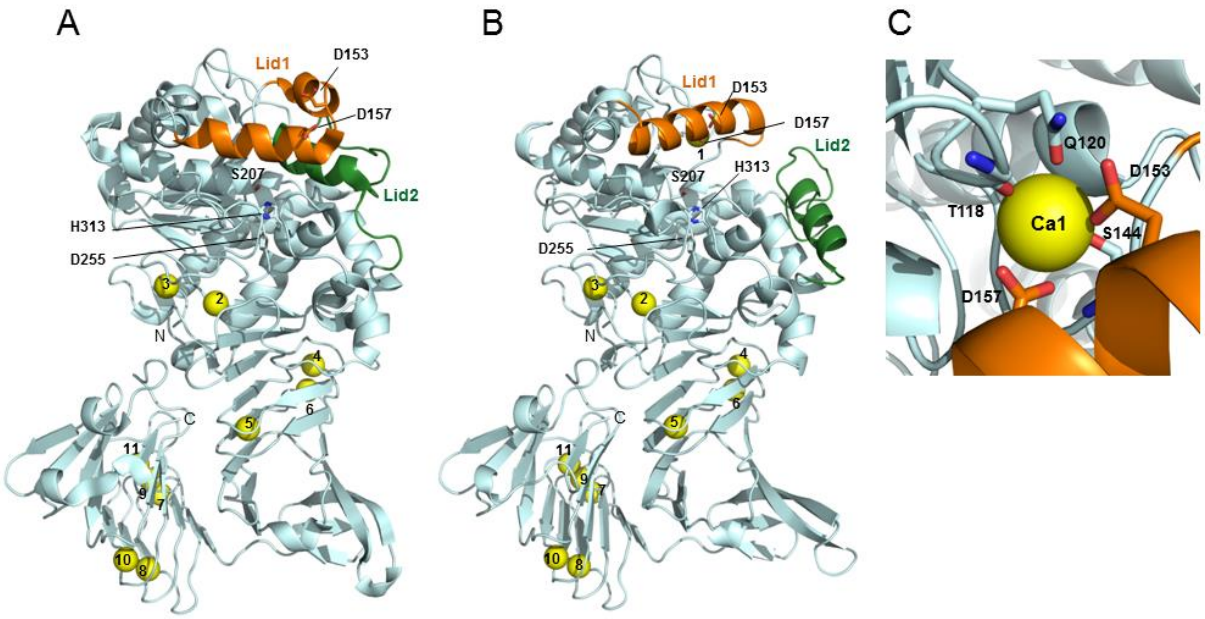

Fig. 3-1. Crystal structures of PML. The entire structures of PML in the closed conformation (PDB ID 2Z8X) (A) and open conformation (PDB ID 2ZVD) (B), and the Ca1 site of PML in the open conformation (C) are shown. The backbone is colored light grey, lid1 is colored orange, and lid2 is colored green. Eleven calcium ions (Ca1-Ca11) are shown as yellow spheres, with their numbers indicated. In panels A and B, the active site residues (Ser207, Asp255 and His313), Asp153, and Asp157 are indicated by stick models, in which oxygen and nitrogen atoms are colored red and blue, respectively. N and C represent the N- and C-termini, respectively. In panel C, the amino acid residues that are coordinated with Ca1 are indicated by stick models, in which oxygen and nitrogen atoms are colored red and blue, respectively.

All mutant proteins were secreted from *E. coli* DH5 cells carrying a heterologous T1SS into the external medium. They were purified to give a single band on SDS-PAGE. The secretion levels of the mutant proteins varied from 20 to 30 mg/L culture and the amounts of the mutant proteins purified from 1 L culture varied from 15 to 25 mg, both of which were comparable to those of PML. The molecular masses of all mutant proteins estimated from gel filtration chromatography (around 68 kDa) were comparable to the calculated one (64.5 kDa), suggesting that they exist as a monomer as does PML.

3.3.2. CD spectra

The far- and near-UV CD spectra of PML and its mutants were measured at pH 8 in the presence of 5mM $CaCl_2$. In this condition, PML assumes a closed conformation (Angkawidjaja *et al*., 2007). The far- and near-UV CD spectra of the several PML mutants (D153R-PML, D153K-PML, and D153R/D157N-PML) are shown in Figures 2A and 2B, respectively, in comparison with those of PML. The far- and near-UV CD spectra of these mutants are highly similar to those of PML, respectively. The far- and near-UV CD spectra of other mutants are not shown, because they were also highly similar to those of PML. These results suggest that the single or double mutations at Asp153 and Asp157 do not significantly affect the overall structure of PML. PML assumes an open conformation in the presence of 5 mM $CaCl_2$ and 0.02% Triton X-100 (Angkawidjaja *et al*., 2010). However, the far- and near-UV CD spectra of PML measured in this condition were highly similar to those measured in the presence of 5 mM $CaCl_2$ and absence of Triton X-100, suggesting that it is difficult to distinguish between the open and closed conformations of PML by CD spectrometry.

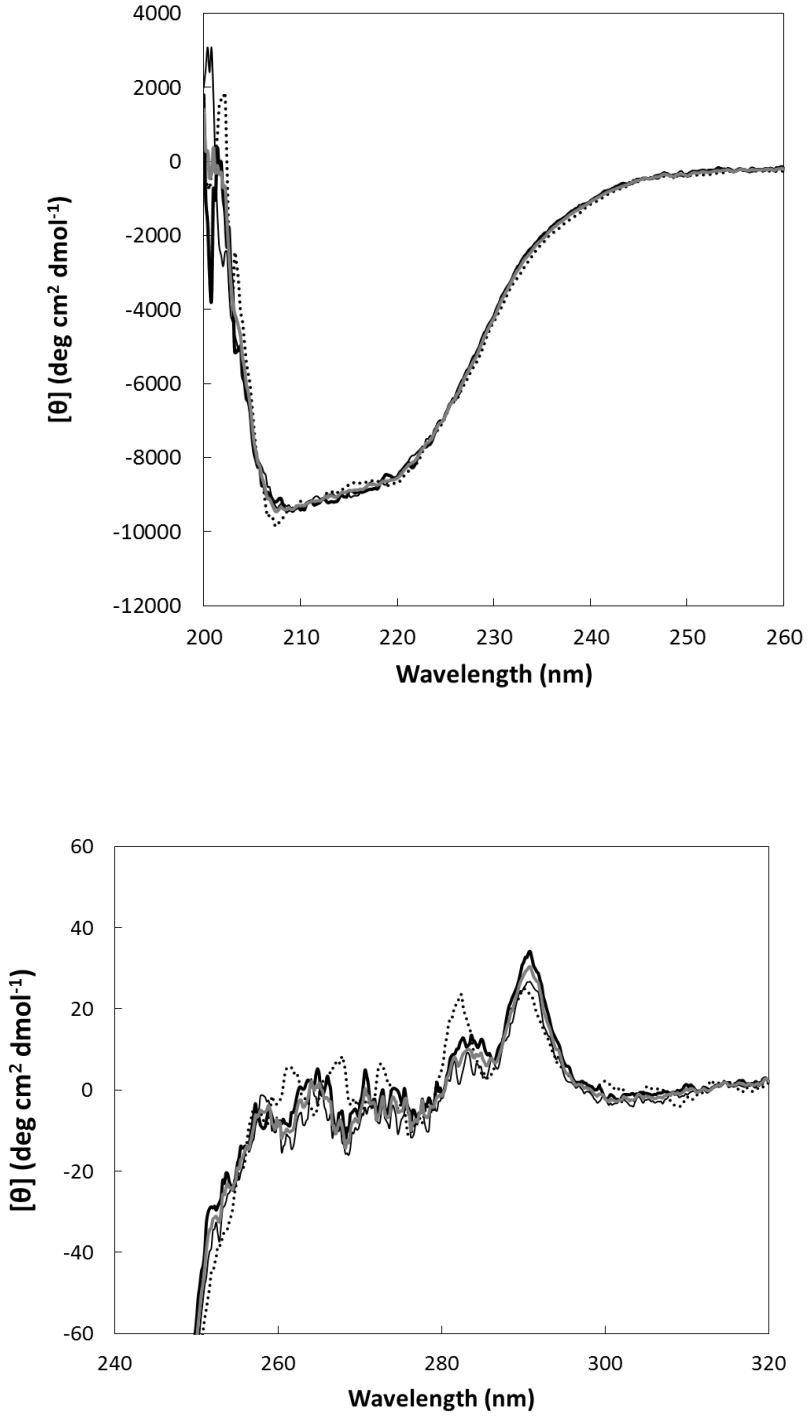

Fig. 3-2. CD Spectra. The far-UV (top) and near-UV (bottom) CD spectra of PML (thick lines), D153R-PML (thin lines), D153K-PML (grey thick lines), and D153R/D157N-PML (dotted lines) are shown. The spectra were measured in the presence of 5 mM $CaCl_2$ at 20°C, as described in Materials and Methods.

3.3.3. Enzymatic activity

Table 3-1. Enzymatic activities of PML and its mutants.

		Esterase[a]		Lipase[a]	
Protein	($CaCl_2$) (mM)	Specific Activity (U/mg)	Relative Activity (%)	Specific Activity (U/mg)	Relative Activity (%)
PML (wild-type)	10	726	100	2725	100
	0	<10	<1.4	<10	<0.4
D153A-PML	10	<10	<1.4	<10	<0.4
	0	<10	<1.4	<10	<0.4
D153K-PML	10	<10	<1.4	<10	<0.4
	0	<10	<1.4	<10	<0.4
D153R-PML	10	417	57.4	890	32.6
	0	500	68.9	450	16.5
D157A-PML	10	<10	<1.4	<10	<0.4
	0	<10	<1.4	<10	<0.4
D157K-PML	10	<10	<1.4	<10	<0.4
	0	<10	<1.4	<10	<0.4
D157R-PML	10	<10	<1.4	<10	<0.4
	0	<10	<1.4	<10	<0.4
D153A/D157A-PML	10	<10	<1.4	<10	<0.4
	0	<10	<1.4	<10	<0.4
D153R/D157N-PML	10	<10	<1.4	<10	<0.4
	0	<10	<1.4	<10	<0.4

[a] The esterase and lipase activities were determined at 30°C in 25 mM Tris-HCl (pH 7.5) in the presence or absence of 10 mM $CaCl_2$ using ethyl-butyrate (C4) and triolein (C18) as a substrate, respectively. The experiment was carried out at least twice and errors from the average values were within 10 and 12% of the values reported for esterase and lipase activities, respectively.

PML assumes an open conformation and therefore exhibits activity in the presence of calcium ions, whereas it assumes a closed conformation and therefore exhibits little activity in the

absence of calcium ions (Kuwahara *et al*., 2008; Angkawidjaja *et al*., 2010). To examine whether the PML mutants assume an open conformation even in the absence of calcium ions, they were dialyzed against calcium-free buffer and their enzymatic activities were determined at pH 7.5 and 30°C in the presence and absence of 10 mM $CaCl_2$. It has been reported that the structure of PML is not significantly changed by this dialysis, although three of the eleven calcium ions bound to the protein (Ca3, Ca6, and Ca10) are removed (Angkawidjaja *et al*., 2010). The lipase and esterase activities of the proteins were determined by using triolein (C18) and ethyl-butyrate (C4) as a substrate, respectively. Of the PML mutants examined, only D153R-PML exhibited lipase and esterase activities even in the absence of calcium ions (Table 3-1). The lipase and esterase activities of D153R-PML in the absence of calcium ions were 7-fold lower and 4-fold higher, respectively, than those of PML in the presence of calcium ions. Other mutants exhibited little lipase and esterase activities either in the presence or absence of calcium ions. These results indicate that lid1 of D153R-PML opens in a calcium-independent manner, whereas that of the other mutants does not open either in the presence or absence of calcium ions.

To examine whether D153R-PML exhibits lower activities toward other triglycerides and higher activities toward other fatty acid ethyl esters than PML, the enzymatic activities of PML and D153R-PML were determined at pH 7.5 and 30°C by using various triglycerides and fatty acid ethyl esters with different acyl chain lengths as substrates. The activities of these proteins toward triglycerides and fatty acid ethyl esters are summarized in Figures 3-3A and 3-3B, respectively. PML was active toward all substrates examined only in the presence of calcium ions. In contrast, D153R-PML was active toward these substrates both in the presence and absence of calcium ions.

When the activities of D153R-PML toward various triglycerides in the absence of calcium ions were compared with those of PML in the presence of calcium ions, the activity of D153R-PML toward triacetin was comparable to that of PML, whereas its activities toward the other triglycerides were lower than those of PML by 2.1-6.8 fold (Fig. 3-3A). When the activities of D153R-PML toward various fatty acid ethyl esters in the absence of calcium ions were compared with those of PML in the presence of calcium ions, the activities of D153R-PML toward ethyl-caproate (C6) and ethyl-laurate (C12) were lower than those of PML by 32 and 12%, respectively, whereas its activities toward ethyl-butyrate (C4), ethyl-caprylate (C8), and ethyl-palmitate (C16)

were higher than those of PML by 3.9, 10.8, and 1.9 fold, respectively (Fig. 3-3B). These results suggest that D153R-PML exhibits lower activity toward most of triglycerides and higher activity toward most of fatty acid ethyl esters than PML. Comparison of the substrate selectivities of D153R-PML and PML indicates that D153R-PML shows the highest preference for triacetin (C2), whereas PML shows a wide preference for triglycerides, with the highest preference for triolein (C18) (Fig. 3-3A). Likewise, D153R-PML shows a wide preference for fatty acid ethyl esters, with the highest preference for ethyl-butyrate (C4), whereas PML shows a strong preference for ethyl-caproate (C6) (Fig. 3-3B). Thus, substrate selectivity of D153R-PML is different from that of PML for both triglycerides and fatty acid ethyl esters. It has been reported that PML shows the highest preference for tributyrin (C4) (Amada *et al*., 2000,Chapter 2). However, the activity of PML toward triolein, which is slightly higher than that toward tributyrin, has not been analyzed previously.

When the activity of D153R-PML in the presence of calcium ions was compared with that in the absence of calcium ions, the activities of D153R-PML toward triacetin (C2), tricaproin (C6), and tricaprylin (C8) in the presence of calcium ions were comparable to those in the absence of calcium ions, whereas the activities of D153R-PML toward tributyrin (C4), triolein (C18) and olive oil in the presence of calcium ions were higher than those in the absence of calcium ions by 2.0-2.9 fold (Fig. 3-3A). However, the activities of D153R-PML toward various triglycerides in the presence of calcium ions were still lower than those of PML by 1.8-4.8 fold. In addition, the activities of D153R-PML toward various fatty acid ethyl esters in the presence of calcium ions were comparable to those in the absence of calcium ions (Fig. 3-3B). These results suggest that Ca1 does not bind to D153R-PML.

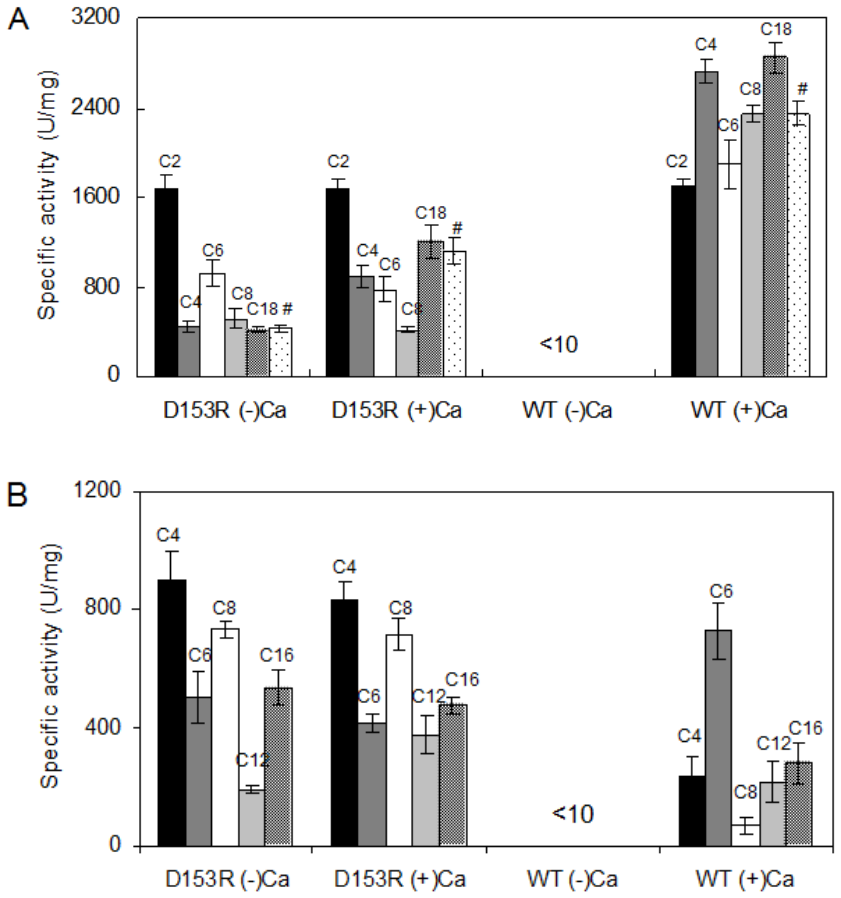

Fig. 3-3. Substrate selectivities of PML and D153R-PML. The specific activities of PML (WT) and D153R-PML (D153R) determined in the absence ((-)Ca) and presence ((+)Ca) of 10 mM $CaCl_2$ using triglycerides (A) and fatty acid ethyl esters (B) with different chain lengths as substrates are shown. C2-C18 represent the acyl chain lengths of the substrates. $C18^{\#}$ represents olive oil. The experiment was carried out in triplicate. Each value represents the average value and errors from the average values are shown.

3.3.4. Interfacial activation

To examine whether D153R-PML undergoes interfacial activation, the activity of D153R-PML was determined at different concentrations of triacetin (C2) in the presence and absence of 10 mM $CaCl_2$. The activity of PML was also determined in the presence of 10 mM $CaCl_2$ for comparative purpose. As shown in Figure 3-4, the plots of these enzymatic activities as a function of triacetin concentration gave sigmoidal curves, indicating that D153R-PML undergoes interfacial activation as does PML. However, the sigmoidal curves of D153R-PML in the presence and absence of calcium ions, which were nearly identical to each other, were different

from that of PML. The activity of PML was greatly enhanced at around critical micellar concentration (CMC) of triacetin (306 mM), as reported previously (Amada *et al*., 2000; Chapter 2). In contrast, the activity of D153R-PML was greatly enhanced at triacetin concentrations higher than CMC.

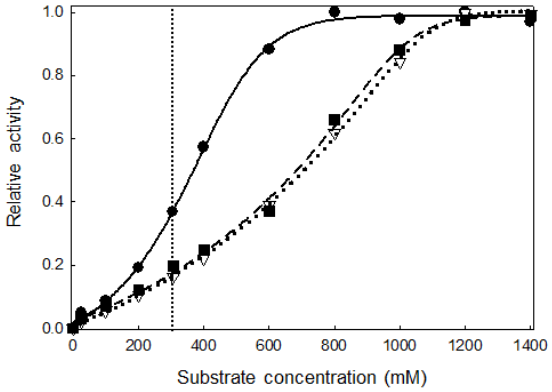

Fig. 3-4. Interfacial activation of PML and D153R-PML. The enzymatic activities of PML determined in the presence of 10 mM $CaCl_2$ (closed circles, straight line), and those of D153R-PML determined in the presence (open triangles, dotted line) and absence (closed squares, dashed line) of 10 mM $CaCl_2$ are shown as a function of triacetin (C_2) concentration. A vertical dotted line represents the CMC of triacetin (C_2), which is 306 mM. The experiment was carried out in duplicate and the errors were within 10% of the values indicated.

3.3.5. Thermal denaturation

To examine whether the mutation of Asp153 to Arg affects the stability of PML, thermal denaturation of PML and D153R-PML was analyzed in the presence or absence of 5 mM $CaCl_2$ and in the presence or absence of 0.02% Triton X-100 by monitoring the change in CD values at 220 nm as the temperature was increased. PML assumes an open conformation only in the presence of calcium ions and Triton X-100 (Angkawidjaja *et al*., 2010), whereas D153R-PML assumes an open conformation in the presence of Triton X-100 either in the presence or absence of calcium ions. The thermal denaturation curves of PML and D153R-PML measured in various conditions are shown in Figure 3-5. The midpoints of the transition of these thermal denaturation curves, $T_{1/2}$, are summarized in Table 2. The $T_{1/2}$ value of D153R-PML is slightly higher than but comparable to that of PML at any condition examined, indicating that the mutation of Asp153 to Arg does not significantly affect the stability of PML, regardless of whether PML assumes an open conformation or a closed conformation.

It is noted that the stability of PML and D153R-PML decreases by 8-9°C in the absence of calcium ions as compared to that in the presence of calcium ions, regardless of whether Triton X-100 is present or not. Eleven calcium ions (Ca1-Ca11) bind to PML in the presence of calcium ions and Triton X-100, whereas eight calcium ions bind to it in the absence of calcium ions and presence of Triton X-100 (Angkawidjaja *et al*., 2010). Ca3, Ca6, and Ca10 are removed from PML in the absence of calcium ions. Of them, Ca3 has been reported to contribute to the stabilization of PML by 5°C (Kuwahara *et al*., 2008). These results suggest that Ca6 and Ca10 contribute to the stabilization of PML by 3-4°C.

Table 3-2. Thermal stabilities of PML and D153R-PML

		$T_{1/2}$ (°C)	
Protein	Triton X-100 (%)	- Ca^{2+}	+ Ca^{2+}
PML	0.02	53.65 ± 0.15	62.46 ± 0.03
	0	53.84 ± 0.61	63.09 ± 0.02
D153R-PML	0.02	54.84 ± 0.15	62.72 ± 0.04
	0	54.62 ± 0.09	63.34 ± 0.03

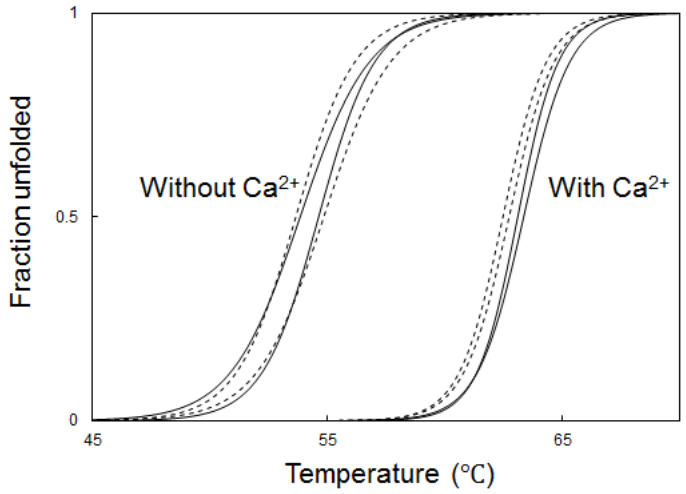

Fig. 3-5. Thermal denaturation curves. Thermal denaturation curves of PML in the presence of 0.02% Triton X-100 (thin dashed lines) and in the absence of Triton X-100 (thin straight lines), and those of D153R-PML in the presence of 0.02% Triton X-100 (thick dashed lines) and in the absence of triton X-100 (thick straight lines) are shown. These curves were measured either in the presence of 5 mM $CaCl_2$ (with calcium) or absence of calcium ions (without calcium). These curves were obtained by monitoring the change in CD values at 220 nm as described in Materials and Methods.

3.4. Discussion

In this study, a PML derivative with calcium-independent activity was successfully constructed by the mutation of Asp153 to Arg. This derivative, D153R-PML, requires calcium ions for folding and its folded structure is probably unchanged by dialysis against calcium-free buffer, as reported for PML (Angkawidjaja *et al*., 2010). Because the activity of D153R-PML is lost by the mutation of Asp157 to Asn, electrostatic attraction between Arg153 and Asp157 seems to be responsible for calcium-independent opening of lid1. Opening of lid1 involves a significant structural change of lid1 from helix-turn-helix to single helix together with rotational and translational movements of lid1 from closed to open positions (Angkawidjaja *et al*., 2010). Arg153 probably facilitates this structural change and movement of lid1 by forming a salt bridge with Asp157. Stabilization of the open conformation of lid by arginine-mediated salt bridges and hydrogen bonds (H-bonds) has also been reported for *Thermomyces lanuginosa* lipase (Brzozowski *et al*., 2000) and *Geobacillus zalihae* lipase (Abdul Rahman *et al*., 2012).

Other PML derivatives designed to introduce an electrostatic attraction between residues 153 and 157, such as D153K-PML, D157R-PML, and D157K-PML, did not exhibit activity either in the presence or absence of calcium ions, probably because the steric configurations of Lys153, Lys157, and Arg157 are not favorable for the formation of this electrostatic attraction. A similar result has been reported for *Staphylococcus hyicus* lipase (SHL). SHL contains a single calcium ion, which is important for stability (Tiesinga *et al*., 2007). Like Asp153 and Asp157 of PML, Asp354 and Asp357 are the only acidic residues that coordinate with this calcium ion. Mutation of Asp357 to Lys, Asn, or Ala resulted in a calcium-independent SHL derivative that retains high stability even in the absence of calcium ion, whereas mutation of Asp354 to Lys or Asn did not (Simons *et al.*, 1999). The steric configurations of Lys354 and Asn354 may be unfavorable for the stabilization of the SHL derivatives.

D153R-PML undergoes interfacial activation like PML. However, the substrate concentration required for this interfacial activation is higher than that required for interfacial activation of PML (Fig. 3-4), indicating that D153R-PML is less sensitive to interfacial activation than PML. This result suggests that the open conformation of D153R-PML is less stable than that of PML. The difference in the anchoring mechanisms of lid1 of D153R-PML and PML may account for this difference. Anchoring of lid1 to the open position of D153R-PML by H-bond

and/or electrostatic interactions may be weaker than that of lid1 to the open position of PML by coordination with Ca1. Because the amount of micellar substrates increases as the substrate concentration increases and because the open conformation of D153R-PML and PML is stabilized by the interaction with micellar substrates, higher substrate concentration is probably required to stabilize the open conformation of D153R-PML than that required to stabilize the open conformation of PML. It has been reported that family I.3 lipase from *Pseudomonas* CR-611 does not undergo interfacial activation, despite the high amino acid sequence identity (93%) to PML (Panizza *et al*., 2013). This result suggests that only a few amino acid substitutions in lid1 affect the sensitivity of family I.3 lipase to interfacial activation.

D153R-PML exhibits lower activity toward triglycerides than PML, with a few exceptions (Fig. 3-3A). This result suggests that the structure and position of lid1 of D153R-PML in the open conformation are different from those of PML. Lid1 is amphiphilic with one side being hydrophilic and containing Arg153 or Asp153 in D153-PML or PML, respectively, and the other side being hydrophobic. The hydrophilic side faces outward and the hydrophobic side faces inward in the closed conformation, whereas the hydrophilic side faces inward and the hydrophobic side faces outward in the open conformation. The hydrophobic side of lid1 in the open conformation is required for binding to micellar substrate. The activities of D153R-PML toward most of the triglycerides decrease as compared to those of PML, probably because the capability of D153R-PML to bind to these substrates decreases as compared to that of PML due to a change in the structure and position of lid1 in the open conformation.

In contrast, D153R-PML exhibits higher activity toward fatty acid ethyl esters than PML, with a few exceptions (Fig. 3-3B). This result suggests that these substrates can access the catalytic pocket of D153R-PML more readily than that of PML. Fatty acid ethyl esters are less hydrophobic and more water-soluble than triglycerides. These substrates exist as monomers or small aggregates, known as pre-micelles (Hadgiivanova *et al*., 2007; Cui *et al*., 2008). Therefore, these substrates may not require full and stable opening of lid1 for their access to the catalytic pocket of the enzyme. D153R-PML exhibits higher activity toward fatty acid ethyl esters than PML, probably because lid1 of D153R-PML more easily opens upon contact with pre-micelles than that of PML due to increased flexibility. The importance of lid for substrate selectivity of lipase has been reported not only for family I.3 lipase (Panizza *et al*., 2013; Chapter 2), but also for other lipases from bacteria (van Kampen *et al*., 1999; Santarossa *et al*., 2005; Secundo *et al*.,

2006), fungi (Holmquist *et al*., 1993; Holmquist *et al*., 1995; Brocca *et al*., 2003; Skjøt *et al*., 2009; Zhu *et al*., 2013), mammal (Yang & Lowe, 2000; Thomas *et al*., 2005), and human (Jennens & Lowe, 1994; Dugi *et al*., 1995; Carrière *et al*., 1997; Bezzine *et al*., 1999). Further structural studies of D153R-PML will be required to understand the mechanism by which D153R-PML exhibits activity in a calcium-independent manner, and the reason why D153R-PML exhibits different substrate selectivity from that of PML.

Because esterase is distinguished from lipase in its ability to catalyze more soluble substrates (Fojan *et al*., 2000), D153R-PML exhibits higher esterase activity than PML. However, D153R-PML is still a true lipase, because it undergoes interfacial activation in a calcium-independent manner. This study is the first study to engineer a family I.3 lipase with calcium-independent activity.

3.5. Summary

A family I.3 lipase from *Pseudomonas* sp. MIS38 (PML) has two lids, lid1 and lid2, which are open when it exhibits activity. A single calcium ion is required to anchor lid1 in the open conformation by coordination with two acidic residues (Asp153 and Asp157) in lid1 and three other residues. Lid1 assumes a long α–helix in the open conformation, whereas it is sharply bent within this helix, such that Asp153 and Asp157 are located far away from each other, in the closed conformation. To examine whether the mutation of Asp153 or Asp157 to a positively-charged residue allows two residues at positions 153 and 157 to come close with each other and thereby stabilizes the open conformation of lid1 even in the absence of calcium ions, five single mutant proteins (D153K-, D153R-, D153A-, D157K-, and D157R-PMLs) and two double mutant proteins (D153A/D157A- and D153R/D157N-PMLs) were constructed. Of these mutant proteins, only D153R-PML exhibited activity in the absence of calcium ions. Its lipase and esterase activities were 7-fold lower and 4-fold higher than those of PML, respectively. These activities were lost by the mutation of Asp157 to Asn. These results suggest that lid1 of D153R-PML opens even in the absence of calcium ions due to electrostatic attraction between Arg153 and Asp157.

CHAPTER 4

General discussion and future remarks

4.1. General discussion

Since lipase is one of the most widely used enzymes in various different sectors, lipase engineering is indispensable to create robust lipase with desired properties for specific application purposes. This is the first study for engineering of a family I.3 lipase with esterase-like activity or calcium-independent activity. Two unique characteristics of PML in particular and family I.3 lipase in general are the presence of two lids that cover the active site, and a catalytically important calcium ion bound to lid1. Lid2 is an auxiliary lid, but apparently plays a major role for interfacial activation of PML. Removal of lid2 does not cause a complete loss of activity. However, PML does not function as a true lipase when lid2 is removed, since PML cannot undergo interfacial activation without lid2 (Fig. 4-1B). Another functional alteration that takes place due to removal of lid2 is a decrease in lipase activity towards triglycerides and an increase in esterase activity towards fatty acid monoesters (Fig. 4-2B). Therefore, lid2 also plays a role in determining substrate specificity and allows PML to act as a lipase, rather than an esterase.

It is well known and accepted that in the open conformation, lid structure exposes its hydrophobic and non-polar amino acid residues to the solvent and by hydrophobic interaction with hydrophobic substrates of lipase, lid structure acts a substrate binding platform for lipase, especially with big and bulky micellar substrates. This is true not only for lid1, but also for lid2, in the case of family I.3 lipase. Therefore, I found and suggested that the hydrophobic surface area which is provided by lid2 is necessary for family I.3 lipase to bind firmly to micellar substrates, since lid1 alone is not sufficient to do so. From engineering point of view, removal of lid2 allows the enzyme to act like esterase than lipase. This information may be useful for lipase engineering, especially with family I.3 lipase, for the engineering of robust catalyst in the production of specific ester compounds.

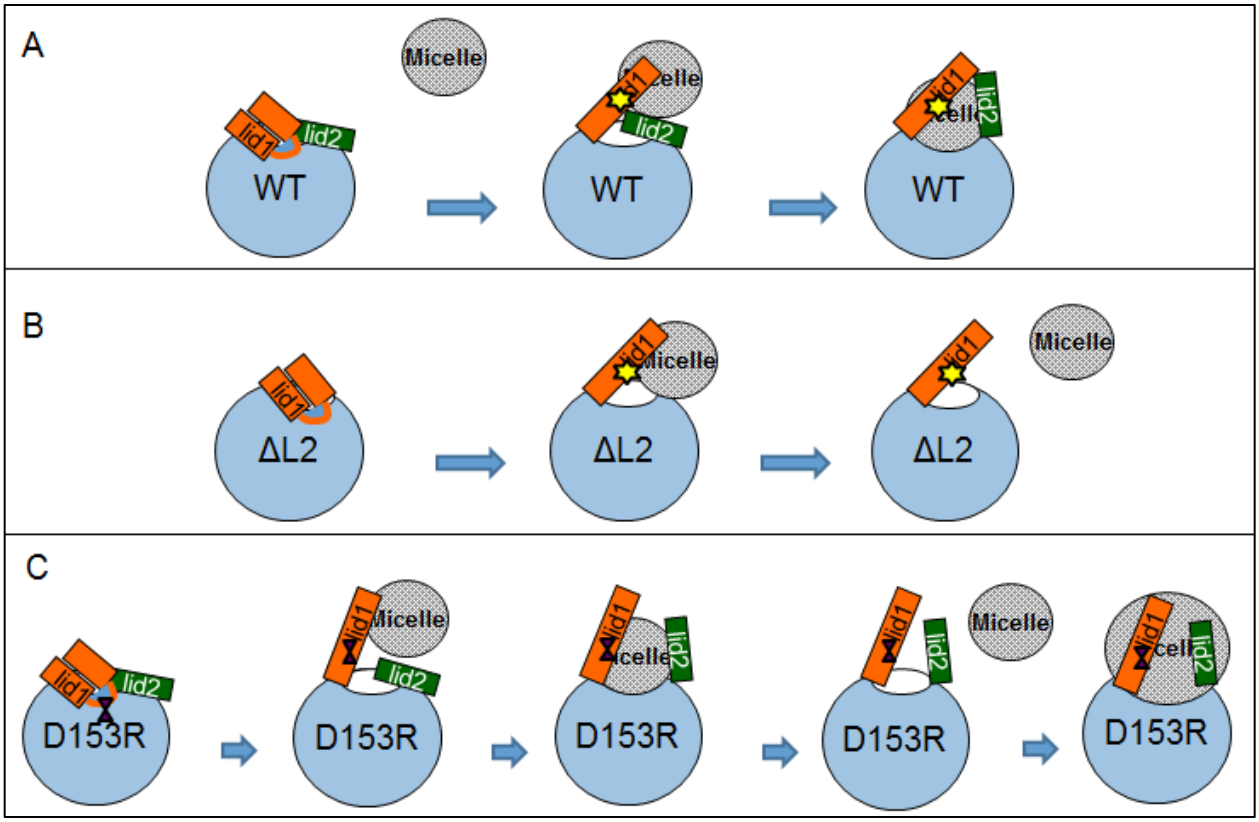

Fig. 4-1. Model figures of the altered enzymatic properties on micellar substrate. (A) Upon contact with micelle, lid1 of PML (WT) opens, followed by lid2. Opening of both lids provides large and continuous hydrophobic surface area for firm attachment to micelle. (B) Lid1 of ΔL2-PML opens upon contact with micelle, but lid1 alone is not enough to attach firmly to micelle. (C) Lid1 of D153R-PML opens in a calcium-independent manner, and the opening of lid1 is different from that of PML (WT), in which bigger and bulkier micelle is necessary for firm attachment of the enzyme to micelle. Lid1 and lid2 are colored orange and green, respectively. Protein body is colored cyan. Ca1 is shown as yellow star. Arg153 is shown as purple double triangle. Catalytic pocket is shown as white ellipse. Micelle is shown as grey circle.

The presence of a metal-ion binding site in the lid of lipase is a unique property for PML and family I.3 lipase. No other class of enzyme has been reported so far which contains calcium ion binding site which is important for catalysis. I exploit this property by engineering a mutant with calcium-independent opening of lid1. While studies on the role of the Ca1 site in stabilizing the open conformation of PML have been conducted, by both mutational study (Kuwahara *et al*., 2008) and in-depth structural analysis with MD simulation (Angkawidjaja *et al*., 2010), the engineering part to remove the Ca1 site in lid1 has not been done before.

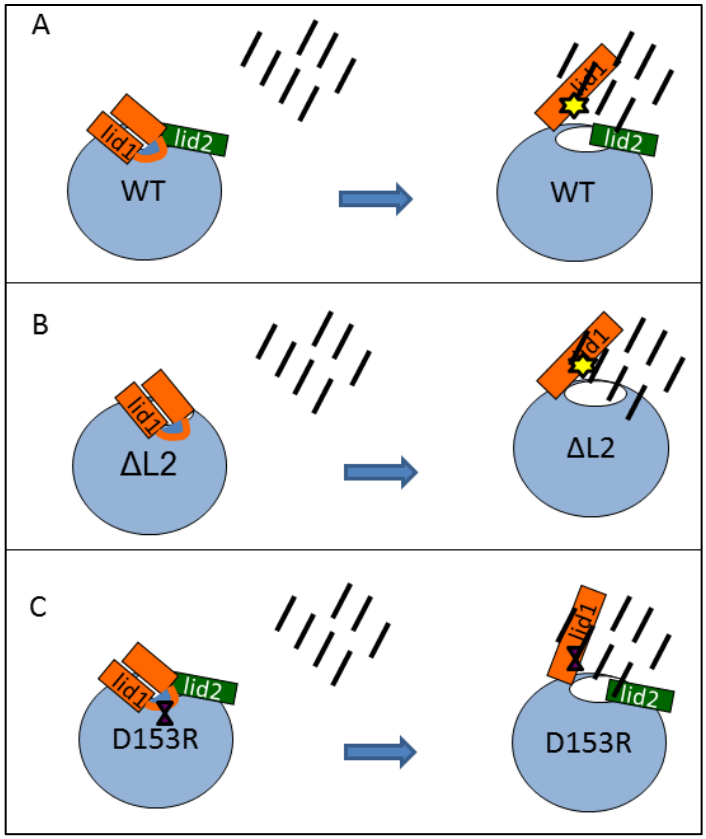

Fig. 4-2. Model figures of the altered enzymatic properties on soluble substrate. (A) Upon contact with substrate, lid1 of PML (WT) opens, but lid2 may not open or only moves a little, thus limiting the access of the substrate to the catalytic pocket. (B) Lid1 of ΔL2-PML (ΔL2) opens upon contact with substrate, allowing access of the substrate to the catalytic pocket, without the hindrance of lid2. (C) Lid1 of D153R-PML (D153R) opens in a calcium-independent manner, and the opening of lid1 is different from that of PML, in which the catalytic pocket is more substrate-accessible, even in the presence of lid2. Lid1 and Lid2 are colored orange and green, respectively. Protein body is colored cyan. Ca1 is shown as yellow star. Arg153 is shown as purple double triangle. Catalytic pocket is shown as white ellipse. Soluble substrates are shown as black lines.

Previous studies have shown that Ca1 provides positive charges necessary to neutralize the negative charge density formed by two closely located aspartate residues (Asp153 and Asp157). Without Ca1, negative charge repulsion occurs when lid1 changes its conformation from closed to open conformations, causing a collapse on lid1, thus inactivating the enzyme because access of the substrate to the active site is blocked by lid1. In this study, I succeeded in obtaining a mutant with calcium-independent activity by mutating Asp153 to Arg (D153R-PML), while mutations at Asp157 and mutation of Asp153 to Lys have proven to be ineffective for such purpose.

D153R-PML mutant is active in the absence of calcium ions, and the mutation also decreases its lipase activity and increases esterase activity as compared to those of PML (Fig. 4-

2C). It also needs substrate concentration higher than CMC. This means that bigger and bulkier micelles are necessary for interfacial activation (Fig. 4-1C). Studies with many other lipases from various sources have shown that a single amino acid substitution in lid can cause such alteration in enzymatic activity and also substrate specificity. This seems to be the same for PML and family I.3 lipase. Since lid is a structural part of lipase that controls the access of the substrate to the active site and is involved in substrate binding, it is obvious that the amino acid sequence of the lid would affects activity and substrate specificity of the enzyme. Until date, there are no other experimental data available on the effect of amino acid substitution at lid1, or lid2 of family I.3 lipase, except for what I presented here in this study.

So far, this is the first study that shows the structural plasticity of the Ca1 site in lid1 of a family I.3 lipase. Destabilization of the protein due to removal of this site by the amino acid substitutions can be overcome by stabilization of the protein due to introduction of a salt bridge between Arg153 and Asp157, thus keeping the lipase active. Other metal ion binding sites in lipase, whether it is catalytically-important or not, can also be engineered by changing the Asp/Asn residue at the metal binding site to positively charged residues such as Arg/Lys.

4.2. Future remarks

Although PML was converted from a true lipase to an esterase-like enzyme by deletion of lid2 and the role of lid2 in PML and family I.3 lipase has been described based on the experimental data and structural analysis on the model structure of the mutant, the crystal structure of ΔL2-PML remains to be solved. By having the crystal structure of the mutant, more accurate and in-depth structural analysis can be done, and it may provide more clues in understanding the structure-function relationships of lid2 and its role in family I.3 lipase. The structure may as well serve as a platform for further rational engineering of family I.3 lipase. The same also goes for D153R-PML, the Ca1-independent mutant. The possibilities that the crystal structure of ΔL2-PML may be different from the modeled one cannot be excluded. Therefore, it would be challenging to solve the structures of both mutants.

Based on the alignment of the amino acid sequences of family I.3 lipases, all members of family I.3 lipase seem to have lid2, as well as the Ca1 site. Mutational studies such as presented in this study can also be performed on other members of family I.3 lipase, to confirm of whether these functional alterations are a general property of family I.3 lipase, or they are unique only to PML.

What can be done further with PML is to exploit its potential applications for production of target compounds. SML, another member of family I.3 lipase, has been implemented in the production of diltiazem, a drug which acts as a calcium channel blocker (Shibatani *et al*., 2000). By utilizing the chemo-, regio-, and enantio-selectivities that PML may possess, purer and shorter steps of production of target compounds can be achieved. For this purpose, studies on the enzymatic activities of PML in micro-aqueous environment, as well as those on its chemo-, regio-, and enantio-selectivities would be indispensable.

References

Abdul Rahman MZ, Salleh AB, Abdul Rahman RN, Abdul Rahman MB, Basri M & Leow TC (2012) Unlocking the mystery behind the activation phenomenon of T1 lipase: a molecular dynamics simulations approach. *Protein Sci* **21**, 1210–1221.

Akatsuka H, Kawai E, Omori K, Komatsubara S, Shibatani T & Tosa T (1994) The lipA gene of *Serratia marcescens* which encodes an extracellular lipase having no N-terminal signal peptide. *J Bacteriol* **176**, 1949–1956.

Amada K, Haruki M, Imanaka T, Morikawa M & Kanaya S (2000) Overproduction in *Escherichia coli*, purification and characterization of a family I.3 lipase from *Pseudomonas sp*. MIS38. *Biochim Biophys Acta* **1478**, 201-210.

Amada K, Kwon HJ, Haruki M, Morikawa M & Kanaya S (2001) Ca^{2+}-induced folding of a family I.3 lipase with repetitive Ca^{2+} binding motifs at the C terminus. *FEBS Lett* **509**, 17-21.

Angkawidjaja C & Kanaya S (2006) Family I.3 lipase: bacterial lipases secreted by the type I secretion system. *Cell Mol Life Sci* **63**, 2804-2817.

Angkawidjaja C, Paul A, Koga Y, Takano K & Kanaya S (2005) Importance of a repetitive nine-residue sequence motif for intracellular stability and functional structure of a family I.3 lipase. *FEBS Lett* **579**, 4707-4712.

Angkawidjaja C, Kuwahara K, Omori K, Koga Y, Takano K & Kanaya S (2006) Extracellular secretion of *Escherichia coli* alkaline phosphatase with a C-terminal tag by type I secretion system: purification and biochemical characterization. *Prot Eng Des Sel* **19**, 337-343.

Angkawidjaja C, You DJ, Matsumura H, Kuwahara K, Koga Y, Takano K & Kanaya S (2007) Crystal structure of a family I.3 lipase from *Pseudomonas sp*. MIS38 in a closed conformation. *FEBS Lett* **581**, 5060-5064.

Angkawidjaja C, Matsumura H, Koga Y, Takano K & Kanaya S (2010) X-ray crystallographic and MD simulation studies on the mechanism of interfacial activation of a family I.3 lipase with two lids. *J Mol Biol* **400**, 82-95.

Arpigny JL & Jaeger KE (1999) Bacterial lipolytic enzymes: classification and properties. *Biochem J* **343**, 177-183.

Bezzine S, Ferrato F, Ivanova MG, Lopez V, Verger R & Carrière F (1999) Human pancreatic lipase: colipase dependence and interfacial binding of lid domain mutants. *Biochemistry* **38**, 5499-5510.

Brocca S, Secundo F, Ossola M, Alberghina L, Carrea G & Lotti M (2003) Sequence of the lid affects activity and specificity of *Candida rugosa* lipase isoenzymes. *Protein Sci* **12**, 2312-2319.

Brzozowski AM, Derewenda U, Derewenda ZS, Dodson GG, Lawson DM, *et al*. (1991) A model for interfacial activation in lipases from the structure of a fungal lipase-inhibitor complex. *Nature* **351**, 491–494.

Brzozowski AM, Savage H, Verma, CS, Turkenburg JP, Lawson DM, Svendsen A & Patkar S (2000) Structural origins of the interfacial activation in *Thermomyces (Humicola) lanuginosa* lipase. *Biochemistry* **39**, 15071–15082.

Cambillau C, Longhi S, Nicolas A & Martinez C (1996) Acyl glycerol hydrolases: inhibitors, interface and catalysis. *Curr Opin Struct Biol* **6**, 449-455.

Carrière F, Thirstrup K, Hjorth S, Ferrato F, Nielsen PF, Withers-Martinez C, Cambillau C, Boel E, Thim L & Verger R (1997) Pancreatic lipase structure-function relationships by domain exchange. *Biochemistry* **36**, 239-248.

Chenal A, Guijarro JI, Raynal B, Delepierre M & Ladant D (2009) RTX calcium binding motifs are intrinsically disordered in the absence of calcium: implication for protein secretion. *J Biol Chem* **284**, 1781-1789.

Chung GH, Lee YP & Rhee JS (1991) Overexpression of a thermostable lipase gene from *Pseudomonas fluorescens* in *Escherichia coli*. *Appl Microbiol Biotechnol* **35**, 237–241.

Collaborative Computational Project, Number 4 (1994) The CCP4 suite: programs for protein crystallography. *Acta Crystallogr D Biol Crystallogr* **50**, 760-763.

Cui X, Mao S, Liu M, Yuan H & Du Y (2008) Mechanism of surfactant micelle formation. *Langmuir* **24**, 10771-10775.

Derewenda U, Brzozowski AM, Lawson DM & Derewenda ZS (1992) Catalysis at the interface: the anatomy of a conformational change in a triglyceride lipase. *Biochemistry* **31**, 1532–1541.

Dugi KA, Dichek HL & Santamarina-Fojo S (1995) Human hepatic and lipoprotein lipase: the loop covering the catalytic site mediates lipase substrate specificity. *J Biol Chem* **270**, 25396-25401.

Emsley P, Lohkamp B, Scott WG & Cowtan K (2010) Features and development of Coot. *Acta Crystallogr D Biol Crystallogr* **66**, 486-501.

Fojan P, Jonson PH, Petersen MT & Petersen SB (2000) What distinguishes an esterase from a lipase: a novel structural approach. *Biochimie* **82**, 1033-1041.

Gill SC & von Hippel PH (1989) Calculation of protein extinction coefficients from amino acid sequence data. *Anal Biochem* **182**, 319-326.

Hadgiivanova R & Diamant H (2007) Premicellar aggregation of amphiphilic molecules. *J Phys Chem B* **111**, 8854-8859.

Hasan F, Shah AA & Hameed A (2006) Industrial applications of microbial lipases. *Enzyme Microb Tech* **39**, 235–251.

Holmquist M, Clausen IG, Patkar S, Svendsen A & Hult K (1995) Probing a functional role of Glu87 and Trp89 in the lid of *Humicola lanuginosa* lipase through transesterification reactions in organic solvent. *J Protein Chem* **14**, 217-224.

Holmquist M, Martinelle M, Berglund P, Clausen IG, Patkar S, Svendsen A & Hult K (1993) Lipases from *Rhizomucor miehei* and *Humicola lanuginosa*: modification of the lid covering the active site alters enantioselectivity. *J Protein Chem* **12**, 749-757.

Horton RM, Cai ZL, Ho SN & Pease LR (1990) Gene splicing by overlap extension: tailor-made genes using the polymerase chain reaction. *Biotechniques* **8**, 528-535.

Jaeger KE & Eggert T (2002) Lipases for biotechnology. *Curr Opin Biotechnol* **13**, 390-397.

Jaeger KE, Dijkstra BW & Reetz MT (1999) Bacterial biocatalysts: molecular biology, three-dimensional structures, and biotechnological applications of lipases. *Annu Rev Microbiol* **53**, 315–351.

Jennens ML & Lowe ME (1994) A surface loop covering the active site of human pancreatic lipase influences interfacial activation and lipid binding. *J Biol Chem* **269**, 25470-25474.

Jiang Z, Zheng Y, Luo Y, Wang G, Wang H, Ma Y & Wei D (2005). Cloning and expression of a novel lipase gene from *Pseudomonas fluorescens* B52. *Mol Biotechnol* **3**, 95–101.

Johnson TL, Abendroth J, Hol WG & Sandkvist M (2006) Type II secretion: from structure to function. *FEMS Microbiol Lett* **255**, 175–186.

Kamil JP, Tischer BK, Trapp S, Nair VK, Osterrieder N & Kung H-J (2005) vLIP, a viral lipase homologue, is a virulence factor of Marek's disease virus. *J Virol* **11**, 6984–6996.

Kim KK, Song HK, Shin DH, Hwang KY & Suh SW (1997) The crystal structure of a triacylglycerol lipase from *Pseudomonas cepacia* reveals a highly open conformation in the absence of a bound inhibitor. *Structure* **5**, 173–185.

Kojima Y, Kobayashi M & Shimizu S (2003) A novel lipase from *Pseudomonas fluorescens* HU380: gene cloning, overproduction, renaturation-activation, two-step purification, and characterization. *J Biosci Bioeng* **96**, 242–249.

Kuwahara K, Angkawidjaja C, Matsumura H, Koga Y, Takano K & Kanaya S (2008) Importance of the Ca^{2+}-binding sites in the N-catalytic domain of a family I.3 lipase for activity and stability. *Protein Eng Des Sel* **21**, 737-744.

Kuwahara K, Angkawidjaja C, Koga Y, Takano K & Kanaya S (2011) Importance of an extreme C-terminal motif of a family I.3 lipase for stability. *Protein Eng Des Sel* **24**, 411-418.

Kwon HJ, Amada K, Haruki M, Morikawa M & Kanaya S (2000) Identification of the histidine and aspartic acid residues essential for enzymatic activity of a family I.3 lipase by site-directed mutagenesis. *FEBS Lett* **483**,139-142.

Kwon HJ, Haruki M, Morikawa M, Omori K & Kanaya S (2002) Role of repetitive nine-residue sequence motifs in secretion, enzymatic activity, and protein conformation of a family I.3 lipase. *J Biosci Bioeng* **93**, 157-164.

Laemmli UK (1970) Cleavage of structural proteins during the assembly of the head of bacteriophage T4. *Nature* **227**, 680-685.

Lee B & Richards FM (1971) The interpretation of protein structures: estimation of static accessibility. *J Mol Biol* **55**, 379-400.

Lee YP, Chung GH & Rhee JS (1993) Purification and characterization of *Pseudomonas fluorescens* SIK W1 lipase expressed in *Escherichia coli*. *Biochim Biophys Acta* **1169**, 156–164.

Li X, Tetling S, Winkler UK, Jaeger KE & Benedik MJ (1995) Gene cloning, sequence analysis, purification, and secretion by *Escherichia coli* of an extracellular lipase from *Serratia marcescens*. *Appl Environ Microbiol* **61**, 2674–2680.

Lindahl E, Hess B & van der Spoel D (2001) GROMACS 3.0: A package for molecular simulation and trajectory analysis. *J Mol Mod* **7**, 306-317.

Matsumae H & Shibatani T (1994) Purification and characterization of the lipase from *Serratia marcescens* Sr41 8000 responsible for asymmetric hydrolysis of 3-phenylglycidic acid esters. *J Ferment Bioeng* **77**, 152–158.

Meier R, Drepper T, Svensson V, Jaeger KE & Baumann U (2007) A calcium-gated lid and a large beta-roll sandwich are revealed by the crystal structure of extracellular lipase from *Serratia marcescens*. *J Biol Chem* **282**, 31477-31483.

Mohamad Ali MS, Mohd Fuzi SF, Ganasen M, Abdul Rahman RN, Basri M & Salleh AB (2013) Structural adaptation of cold-active RTX lipase from *Pseudomonas* sp. strain AMS8 revealed via homology and molecular dynamics simulation approaches. *BioMed Res Int*, http://dx.doi.org/10.1155/2013/925373.

Nardini M & Dijkstra BW (1999) α/β hydrolase fold enzymes: the family keeps growing. *Curr Opin Struct Biol* **9**, 732-737.

Oh B, Kim H, Lee J, Kang S & Oh T (1999) *Staphylococcus haemolyticus* lipase: biochemical properties, substrate specificity and gene cloning. *FEMS Microbiol Lett* **179**, 385–392.

Omori K, Idei A & Akatsuka H (2001) *Serratia* ATP-binding cassette protein exporter, Lip, recognizes a protein region upstream of the C terminus for specific secretion. *J Biol Chem* **267**, 27111-27119.

Panizza P, Syfantou N, Pastor FIJ, Rodríguez S & Díaz P (2013) Acidic lipase Lip I.3 from a *Pseudomonas fluorescens*-like strain displays unusual properties and shows activity on secondary alcohols. *J Appl Microbiol* **114**, 722–732.

Papaleo E & Invernizzi G (2011) Conformational plasticity of the calcium-binding pocket in the *Burkholderia glumae* lipase: remodeling induced by mutation of calcium coordinating residues. *Biopolymers* **95**, 117–126.

Potterton E, Briggs P, Turkenburg M & Dodson E (2003) A graphical user interface to the CCP4 program suite. *Acta Crystallogr D Biol Crystallogr* **59**, 1131-1137.

Rashid N, Shimada Y, Ezaki S, Atomi H & Imanaka, T (2001) Low-temperature lipase from psychrotrophic *Pseudomonas* sp. strain KB700A. *Appl Environ Microbiol* ***67***, 4064–4069.

Saff EB & Kuijlaars ABJ (1997) Distributing many points on a sphere. *Math Intelligencer* **19**, 5-11.

Santarossa G, Lafranconi PG, Alquati C, DeGioia L, Alberghina L, Fantucci P & Lotti M (2005) Mutations in the "lid" region affect chain length specificity and thermostability of a *Pseudomonas fragi* lipase. *FEBS Lett* **579**, 2383-2386.

Secundo F, Carrea G, Tarabiono C, Gatti-Lafranconi P, Brocca S, Lotti M, Jaeger KE & Eggert T (2006) The lid is a structural and functional determinant of lipase activity and selectivity. *J Mol Cat B: Enz* **39**, 166–170.

Shibatani T, Omori K, Akatsuka H, Kawai E & Matsumae H (2000) Enzymatic resolution of diltiazem intermediate by *Serratia marcescens* lipase: molecular mechanism of lipase secretion and its industrial application. *J Mol Catal B: Enzymatic* **10**, 141–149.

Simons JW, van Kampen MD, Ubarretxena-Belandia I, Cox RC, Alves dos Santos CM, Egmond MR & Verheij HM (1999) Identification of a calcium binding site in *Staphylococcus hyicus* lipase: generation of calcium-independent variants. *Biochemistry* **38**, 2–10.

Skjøt M, De Maria L, Chatterjee R, Svendsen A, Patkar SA, Ostergaard PR & Brask J (2009) Understanding the plasticity of the α/β hydrolase fold: lid swapping on the *Candida antarctica* lipase B results in chimeras with interesting biocatalytic properties. *Chembiochem* **10**, 520-527.

Sotomayor Pérez AC, Karst JC, Davi M, Guijarro JI, Ladant D & Chenal A (2010) Characterization of the regions involved in the calcium-induced folding of the intrinsically disordered RTX motifs from the *Bordetella pertussis* adenylate cyclase toxin. *J Mol Biol* **397**, 534-549.

Stehr F, Kretschmar M, Kröger C, Hube B & Schäfer W (2003) Microbial lipases as virulence factors. *J Mol Catal B: Enzymatic* **22**, 347–355.

Svendsen A, Borch K, Barfoed M, Nielsen TB, Gormsen E & Patkar SA (1995) Biochemical properties of cloned lipases from the *Pseudomonas* family. *Biochim Biophys Acta* **1259**, 9–17.

Talon R, Dublet N, Montel MC & Cantonnet M (1995) Purification and characterization of extracellular *Staphylococcus warneri* lipase. *Curr Microbiol* **30**, 11–16.

Tan Y & Miller KJ (1992) Cloning, expression, and nucleotide sequence of a lipase gene from *Pseudomonas fluorescens* B52. *Appl Environ Microbiol* **58**, 1402–1407.

Tanaka A, Sugimoto H, Muta Y, Mizuno T, Senoo K, Obata H & Inouye K (2003) Differential scanning calorimetry of the effects of Ca^{2+} on the thermal unfolding of *Pseudomonas cepacia* lipase. *Biosci Biotechnol Biochem* **67**, 207–210.

Thomas A, Allouche M, Basyn F, Brasseur R & Kerfelec B (2005) Role of the lid hydrophobicity pattern in pancreatic lipase activity. *J Biol Chem* **280**, 40074-40083.

Thompson JD, Higgins DG & Gibson TJ (1994) CLUSTAL W: improving the sensitivity of progressive multiple sequence alignment through sequence weighting, position specific gap penalties and weight matrix choice. *Nucleic Acids Res* **22**, 4673–4680.

Tiesinga JJW, van Pouderoyen G, Nardini M, Ransac S & Dijkstra BW (2007) Structural basis of phospholipase activity of *Staphylococcus hyicus* lipase. *J Mol Biol* **371**, 447–456.

van Kampen MD, Verheij HM & Egmond MR (1999) Modifying the substrate specificity of Staphylococcal lipases. *Biochemistry* **38**, 9524-9532.

van Tilbeurgh H, Egloff M-P, Martinez C, Rugani N, Verger R, *et al*. (1993) Interfacial activation of the lipase-procolipase complex by mixed micelles revealed by X-ray crystallography. *Nature* **362**, 814–820.

Verger R (1997) 'Interfacial activation' of lipases: facts and artifacts. *Trends Biotechnol* **15**, 32–38

Yang J, Kobayashi K, Iwasaki Y, Nakano H & Yamane T (2000) In vitro analysis of roles of a disulfide bridge and a calcium binding site in activation of *Pseudomonas* sp. strain KWI-56 lipase. *J Bacteriol* **182**, 295–302.

Yang Y & Lowe ME (2000) The open lid mediates pancreatic lipase function. *J Lipid Res* **41**, 48-57.

Zhu S-S, Li M, Yu X & Xu Y (2013) Role of Met93 and Thr96 in the lid hinge region of *Rhizopus chinensis* lipase. *Appl Biochem Biotechnol* **170**, 436–447.

List of publications

1. Cheng,M., Angkawidjaja,C., Koga,Y., Kanaya,S. (2012) Requirement of lid2 for interfacial activation of a family I.3 lipase with unique two lid structures. *FEBS J.*, 279, 3727–3737.
2. Cheng,M., Angkawidjaja,C., Koga,Y., Kanaya,S. (2014) Calcium-independent opening of lid1 of a family I.3 lipase by a single Asp to Arg mutation at the calcium-binding site. *Prot. Eng. Des. Sel.* in press. DOI: 10.1093/protein/gzu009

Acknowledgements

I praise God Almighty, Creator of Heaven and Earth for His endless provision and blessings on me. I acknowledge that it is not by my own power, but it is His hands that brought me to Japan in the first place, and got me through all the way until I can graduate and get a doctoral degree. The very same hands that will also deliver me throughout everything else that I may face in the future. Praise the Lord, for He is good!

I would like to express the deepest appreciation and my deepest gratitude to my supervisor whom also the committee chair Professor Shigenori Kanaya. He continually and convincingly conveyed a spirit of adventure, excitement and perfection in regard to research, and passion in regard to teaching. Without his guidance and persistent help this dissertation would not have been possible. He also continuously provided the support and recommendation for my doctoral scholarship application, which without I would not be able to get any scholarship. I really appreciate his understanding and patience, especially when I was pregnant. Prof. Kanaya is not just a figure in research, but he is also a teacher who really cares for his students. I believe every other international student in Kanaya Lab would agree with me on this.

A very special thanks to Assistant Professor Clement Angkawidjaja, who kindly helped me to get to know Kanaya Lab, and supervised me day by day when I just started my research and had not get a grasp on what I got to do next. His insights and suggestions really had helped me a lot throughout the challenges and difficulties that I faced in my research. His contribution to my graduation is indispensable, and I am grateful that I met a mentor/ supervisor like him. I am also grateful for all the advices, and help he gave in other aspects beside research work.

I also thank Prof. Kazufumi Takano, Associate Prof. Yuichi Koga for their suggestions, advices and comments on my reports, experimental data and methods. I thank Associate Prof. Yuichi Koga for picking me up and took me with his car to the dormitory where I had stayed, and for his friendliness throughout my study in Kanaya Lab. My thanks also go to Dr. Eiko Kanaya for her advices and comments on my work, and for her smiles and kindness.

To Mrs. Reiko Matsumoto, I offer my sincere gratitude for always being there to provide helping hands in terms of administration and paperwork, especially those in Japanese. Being careful and always pay attention to details are her quality that makes her excelled in her job as a lab secretary. How I am grateful that Kanaya Lab had Mrs. Matsumoto as the lab secretary, especially during my first year in Japan, when all things in Japanese were troublesome to me. The last but not the least, for her friendliness, kindness and her delicious food, cakes and desserts, I am thankful to her.

To my family, especially my husband and my little baby who have been with me through all the process, words alone cannot explain how grateful I am, being blessed with your presence in my life. The help and encouragement you both provided for me had helped me through it all.

Finally, I owe my gratitude to fellow Kanaya Lab members, Japanese and International students. Thanks to the warm welcome and help from my Japanese seniors; Okamoto Tomohiro, Nishio Sayaka, and Dr. Kuwahara. To Dr. Cahyo Budiman, I am grateful for his friendship and his advices. Special thanks to Dr. Nguyen Tri Nhan, Dr. Nujarin Jongruja, Elias Tannous, Sintawee Sulaiman and Etin Dyah Permatasari for all the laughter we shared, and for all the help and supports. I cherish the time I spent with you, and may fate bring us together again someday in the future.